Chemical Research in Toxicology

ACS AuthorChoice

Article

pubs.acs.org/crt

Terms of Use

Biochemical Analysis of Six Genetic Variants of Error-Prone Human DNA Polymerase ι Involved in Translesion DNA Synthesis

Jinsook Kim,[†] Insil Song,[†] Ara Jo,[†] Joo-Ho Shin,[†] Hana Cho,[‡] Robert L. Eoff,[§] F. Peter Guengerich,[∥] and Jeong-Yun Choi*,[†]

[†]Division of Pharmacology, Department of Molecular Cell Biology, and [‡]Department of Physiology, Samsung Biomedical Research Institute, Sungkyunkwan University School of Medicine, Suwon, Gyeonggi-do 440-746, Republic of Korea

[§]Department of Biochemistry and Molecular Biology, University of Arkansas for Medical Sciences, Little Rock, Arkansas 72205-7199, United States

[∥]Department of Biochemistry and Center in Molecular Toxicology, Vanderbilt University School of Medicine, Nashville, Tennessee 37232-0146, United States

Supporting Information

ABSTRACT: DNA polymerase (pol) ι is the most error-prone among the Y-family polymerases that participate in translesion synthesis (TLS). Pol ι can bypass various DNA lesions, e.g., N^2-ethyl(Et)G, O^6-methyl(Me)G, 8-oxo-7,8-dihydroguanine (8-oxoG), and an abasic site, though frequently with low fidelity. We assessed the biochemical effects of six reported genetic variations of human pol ι on its TLS properties, using the recombinant pol ι (residues 1−445) proteins and DNA templates containing a G, N^2-EtG, O^6-MeG, 8-oxoG, or abasic site. The Δ1−25 variant, which is the *N*-terminal truncation of 25 residues resulting from an initiation codon variant (c.3G > A) and also is the formerly misassigned wild-type, exhibited considerably higher polymerase activity than wild-type with Mg^{2+} (but not with Mn^{2+}), coinciding with its steady-state kinetic data showing a ∼10-fold increase in k_{cat}/K_m for nucleotide incorporation opposite templates (only with Mg^{2+}). The R96G variant, which lacks a R96 residue known to interact with the incoming nucleotide, lost much of its polymerase activity, consistent with the kinetic data displaying 5- to 72-fold decreases in k_{cat}/K_m for nucleotide incorporation opposite templates either with Mg^{2+} or Mn^{2+}, except for that opposite N^2-EtG with Mn^{2+} (showing a 9-fold increase for dCTP incorporation). The Δ1−25 variant bound DNA 20- to 29-fold more tightly than wild-type (with Mg^{2+}), but the R96G variant bound DNA 2-fold less tightly than wild-type. The DNA-binding affinity of wild-type, but not of the Δ1−25 variant, was ∼7-fold stronger with 0.15 mM Mn^{2+} than with Mg^{2+}. The results indicate that the R96G variation severely impairs most of the Mg^{2+}- and Mn^{2+}-dependent TLS abilities of pol ι, whereas the Δ1−25 variation selectively and substantially enhances the Mg^{2+}-dependent TLS capability of pol ι, emphasizing the potential translational importance of these pol ι genetic variations, e.g., individual differences in TLS, mutation, and cancer susceptibility to genotoxic carcinogens.

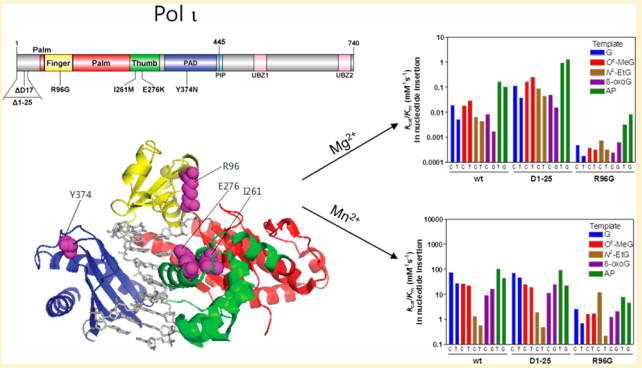

INTRODUCTION

DNA damage is constantly generated from endogenous and exogenous sources in cells and poses a major obstacle to vital cellular processes of replication and transcription, possibly leading to mutation and cell death. To cope with the constant threat of DNA damage, cells are equipped with a sophisticated network of DNA damage response systems, including DNA repair mechanisms, damage tolerance processes, and cell-cycle checkpoints.[1,2] Such systems should ideally have high fidelity, efficiency, and coordination with each other to preserve genome integrity, but these properties are not perfect nor the same for all lesions. Sometimes the attempts at repair can result in genomic errors and cell apoptosis. Inherited defects in human DNA damage response machineries (e.g., XPC, POLH, ATM) cause the faulty repair, damage tolerance, and checkpoints and commonly result in severe cancer predisposition disorders along with other different disease phenotypes.[3,4] Reduced DNA repair capacity and related genetic variations have been shown to be associated with enhanced cancer risks in human individuals.[5−8] Along the same line, it can be speculated that the differential cellular capacity for DNA damage tolerance influences the final biological outcomes from residual genomic lesions and thus could be a determining factor for mutation and cancer predisposition in individuals.

Received: July 9, 2014
Published: August 27, 2014

   dx.doi.org/10.1021/tx5002755 | *Chem. Res. Toxicol.* 2014, 27, 1837−1852

Persistent unrepaired DNA lesions can interfere with DNA replication, which can lead to replication fork stalling and copying errors. As a prompt response to the lesion-blocked replication fork, cells are able to utilize a DNA damage tolerance system involving specialized translesion polymerases, mostly belonging to the Y-Family, which overcomes DNA lesions and performs translesion synthesis (TLS). TLS is a potentially mutagenic process due to the low fidelity of TLS polymerases with lesions in many cases, while serving to avoid the permanent cell cycle arrest and cell death. Indeed, each Y-Family polymerase can carry out its unique TLS, varying in both efficiency and fidelity depending on the type, size, and location of the lesion.[9] Therefore, individual TLS polymerases may play distinctive roles, i.e., protective (error-free), provocative (error-prone), or neutral, in mutagenesis induced by each specific DNA lesion in cells. For instance, both pol κ and REV1 can perform error-free and efficient TLS at bulky N^2-guanine (G) lesions, such as benzo[*a*]pyrene-derived N^2-G adducts but pol η and pol ι perform relatively error-prone TLS (albeit yielding different types of errors) at those adducts,[10−13] suggesting error-free roles for the former two pols but error-prone roles for the latter two pols in TLS (at least regarding bulky carcinogen-bound N^2-G adducts). In these circumstances, it can be postulated that the overall cellular TLS capacity, comprising behaviors of multiple individual polymerases employed against carcinogen-specific DNA lesions, will determine the levels of lesion-derived mutations in the newly synthesized genome and thus play a role in preventing or facilitating mutagenesis resulting from genotoxic carcinogens in cells, which could further relate to cancer susceptibility in individuals.

DNA polymerase (pol) ι, a member of human Y-family DNA polymerases, has been known to perform TLS at various DNA lesions although it has the lowest fidelity in DNA synthesis among polymerases. Pol ι is inherently very error-prone in nucleotide insertion, particularly opposite undamaged template bases G and T, respectively, yielding misinsertion of either dTTP or dGTP at a frequency of about 0.1 and 1 (relative to the correct nucleotide insertion), which is ascribed to its unique active site and related non-Watson−Crick base pairing.[14−16] Pol ι is able to mediate relatively mutagenic but occasionally accurate replicative bypass with a variety of DNA lesions, including minor-groove N^2-G adducts, major-groove O^6-G adducts, 8-oxo-7,8-dihydroG (8-oxoG), pyrimidine dimers, and abasic lesions, with different nucleotide selectivities according to lesion types. Pol ι inserts both dCTP and dTTP opposite N^2-G and O^6-G adducts, with a slight preference of either dCTP or dTTP, respectively.[17] Pol ι slightly prefers dCTP over dGTP for insertion opposite 8-oxoG, prefers dATP opposite the 3′ T (but both dGTP and dTTP opposite 5′ T) of (6−4) TT photoproducts, and slightly prefers to insert dTTP and dGTP opposite abasic lesions.[18,19] Pol ι is distinctively known to prefer Mn^{2+} over Mg^{2+} ions as a metal in polymerase catalysis and is maximally active at low concentrations (0.05−0.25 mM) of Mn^{2+}.[20]

Substantial evidence suggests a possible implication of pol ι in cancer in mammals. Pol ι deficiency results in a higher susceptibility to UV-induced skin cancers in mice under pol η-null conditions,[21,22] and the loss of pol ι increases urethane-induced lung mutagenesis and tumorigenesis in C57BL/6J pol ι-knockout mice.[23] Dysregulation of pol ι is also found in many types of cancers. Pol ι is overexpressed in various types of cancerous tissues or cells including breast, prostate, uterus, stomach, rectal, esophageal, and bladder cancers,[24−27] which might hypothetically lead to a mutator phenotype due to an elevated error-prone DNA replication. Two germline *POLI* single nucleotide variations (SNVs), which might result in a missense change at codon 532 or 731 located in the ubiquitin-binding motifs, have been associated with a significantly higher risk of some subsets of lung and prostate cancers, respectively, although their specific mechanisms have not been elucidated yet.[28,29] On the basis of these circumstances, we can infer that pol ι would serve a protective (or sometimes facilitative) role in genomic mutagenesis induced by genotoxic agents in cells, and the altered status of pol ι function by genetic variation might affect individual risks of mutation and cancer from exposure to certain genotoxic carcinogens.

The human *POLI* gene encodes the pol ι protein consisting of 740 amino acids according to NCBI GenBank database (http://www.ncbi.nlm.nih.gov/genbank/), which has the additional N-terminal 25 residues to the formerly erroneously designated open-reading frame (ORF) amino acid sequence. For such a reason, most of the previous biochemical and structural experiments on pol ι were performed using the sequence information on the N-terminal truncated (25-amino acids-shorter) ORF. The catalytic core of pol ι is positioned in the N-terminal region (amino acids 26−445), and its ternary complex crystal structure has been determined.[14] However, biochemical properties of the new wild-type pol ι, as well as the effect of the extra 25 amino acids (containing 12 acidic residues) added at the N-terminus, on pol ι function, have not been reported. Until the present time, a total of ∼122 germline variations in *POLI* gene have been described for human individuals in dbSNP (http://www.ncbi.nlm.nih.gov/projects/SNP), but the functional impacts of these genetic variations have not been biochemically evaluated yet. Biochemical approaches to evaluate the effects of germline genetic variations on pol ι function are indispensable for understanding and predicting their mechanistic basis and biological outcomes either before or after studying their clinical associations. In this study, we focused on the nonsynonymous coding *POLI* gene variations, which are located in the polymerase core domains and the N-terminal 25 amino acids region, and predicted to have damaging effects by *in silico* prediction analysis tools, e.g., SIFT and PolyPhen,[30−32] because they would be likely to affect the catalytic function of pol ι and change its TLS function. In order to characterize the putatively functional genetic variations of human pol ι, we investigated the biochemical effects of six selected missense or deletion genetic variations on the enzymatic properties of human pol ι regarding both normal DNA synthesis and bypass of various DNA lesions. We performed the experiments with "standing-start" full-length primer extensions, steady-state kinetics, and pol-DNA binding in the presence of either Mg^{2+} or Mn^{2+} ions, using wild-type recombinant human pol ι (1−445 amino acids) and six variants with primer-annealed oligonucleotide DNA templates containing an undamaged G, N^2-ethyl(Et)G, O^6-methyl(Me)G, 8-oxoG, or abasic site. Here we describe two germline genetic variations that can alter *in vitro* enzyme function of pol ι in nucleotide incorporation with normal and lesion DNA substrates, as well as DNA substrate binding. These observations are discussed in the context of understanding the possible mechanistic and functional aspects of altered TLS with pol ι variants.

Table 1. *POLI* Gene Variations Studied

rs ID[a]	nucleotide change	amino acid change	protein domain	minor allele frequency	prediction[b]	
					SIFT	PolyPhen-2
rs199757163	c.3G > A	M1_A25del (Δ1−25)[c]		0.001[d]	N/A[e]	N/A
rs10584411	c.51_53del	D17del (ΔD17)		0.747[d]	N/A	N/A
rs3218778	c.286A > G	R96G	finger	0.006[f]	damaging	probably damaging
rs3218784	c.783A > G	I261M	thumb	0.011[d]	damaging	possibly damaging
rs3218783	c.826G > A	E276K	thumb	0.0005[d]	damaging	possibly damaging
rs11558769	c.1120T > A	Y374N	PAD	N/A	damaging	benign

[a]A reference SNP identification number provided by dbSNP. [b]Possible functional effects of genetic variations are predicted *in silico* using SIFT and PolyPhen-2.[30−32] [c]The Greek symbol Δ denotes a deletion. [d]From 1000 Genomes project. [e]Not available. [f]From NIHPDR and PDR90 resources described in dbSNP.

EXPERIMENTAL PROCEDURES

Materials. T4 polynucleotide kinase, restriction endonucleases, and dNTPs were purchased from New England Biolabs (Ipswich, MA). [γ-^{32}P]ATP (specific activity 3 × 10^3 Ci/mmol) was purchased from PerkinElmer Life Sciences (Boston, MA). Biospin columns were purchased from Bio-Rad (Hercules, CA). A protease inhibitor cocktail was obtained from Roche Applied Science (Indianapolis, IN). The vector pBG101 was gratefully obtained from the Center for Structural Biology, Vanderbilt University. The pCR2.1-TOPO TA cloning kit was from Invitrogen (Carlsbad, CA), and the QuickChange mutagenesis kit was from Stratagene (La Jolla, CA). FPLC columns were purchased from GE Healthcare (Uppsala, Sweden).

DNA Substrates. 24-Mer (5′-GCC TCG AGC CAG CCG CAG ACG CAG-3′) and 36-mer (3′-CGG AGC TCG GTC GGC GTC TGC GTC XCT CCT GCG GCT-5′; X = G, O^6-MeG, or tetrahydrofuran (abasic site analogue)) oligonucleotides containing a G, O^6-MeG, or abasic site (stable tetrahydrofuran derivative) were obtained from Midland Certified Reagent Co. (Midland, TX). A 36-mer (X = N^2-EtG) containing N^2-EtG was prepared as previously described.[33] A 36-mer (X = 8-oxoG) containing an 8-oxoG, and an 18-FAM-mer (5′-(FAM)-AGC CAG CCG CAG ACG CAG-3′; FAM = 6-carboxyfluorescein) were obtained from Bioneer (Daejeon, Korea). Primers (24-mers) were 5′ end-labeled using T4 polynucleotide kinase with [γ-^{32}P]ATP and annealed with 36-mer templates to make duplex primer-template DNA substrates for use in polymerase activity assays. 18-FAM-mer primers were annealed with 36-G-mer templates for use in DNA binding assays.

Selection of Human *POLI* Gene Variations Having Potentially Functional Impact. We searched for human *POLI* gene variations that are highly likely to alter enzyme function. First, we screened the naturally occurring germ-line genetic variations in the protein-coding sequence of the *POLI* gene from the public database dbSNP (http://www.ncbi.nlm.nih.gov/projects/SNP). We selected four candidate variations to be likely dysfunctional based on three criteria: (i) nonsynonymous coding variations that cause a missense or nonsense change, (ii) variations located in the polymerase core domain (amino acid residues 1 to 445), and (iii) missense variations predicted to be deleterious or damaging on protein function by SIFT and Polyphen.[30−32] We also included two more candidate variations, which cause the initiation codon change or an amino acid deletion and thus might exert functional changes. Thus, we selected six variants (i.e., a deletion, an initiator codon, and four missense variants) and performed detailed biochemical analyses using the corresponding recombinant protein pol ι^{1-445} proteins purified from *Escherichia coli*. Current information for the six *POLI* gene variations included in this study is summarized in Table 1, based on public databases, e.g., dbSNP, 1000 genomes (http://browser.1000genomes.org).

Construction of Expression Vectors for Core Proteins of Wild-type Pol ι and Six Variants. The gene fragments covering the core proteins (amino acids 1−445) of wild-type pol ι and the Δ1−25 variant were obtained by PCR amplification from human testis cDNA (Clontech, Mountain View, CA) as template using AccuTaq LA DNA polymerase (Sigma, St. Louis, MO) with a forward primer (5′-GAA TCC ATG GAG AAG CTG GGG GTG G-3′ for wild-type or 5′-GAA TCC ATG GAG TCG GCA GAG GGT GTG-3′ for Δ1−25) and a reverse primer (5′-CTA CTT AGC AGT ATT TAG TGC-3′). Each of the resulting PCR products of 1.3 kb *POLI core* was cloned into the vector pCR2.1-TOPO, and the nucleotide sequences of pol ι gene inserts for wild-type and Δ1−25 were confirmed. From the nucleotide sequencing of wild-type gene inserts, we obtained two kinds of vectors encoding the wild-type or ΔD17 variant pol ι(1−445), indicating that ΔD17 variation is very common in the human population. Each of the *POLI* gene fragments were then cloned into the *Bam*HI and *Eco*RI sites of the vector pBG101, which can generate the pBG101-wtPOLI$^{1-445}$, and two vectors encoding the Δ1−25 or ΔD17 pol ι(1−445) variant. Each of the four different mutations in the *POLI* gene was created by a QuickChange mutagenesis kit with the pBG101-wtPOLI$^{1-445}$ vector as template. The oligonucleotide primers for introducing the point mutations in *POLI* were 5′-GGT TAC CTG CAA CTA TGA AGC TGG GAA ACT TGG AG-3′ for R96G, 5′-CTT ATT CAT AGT TTG AAT CAC ATG AAG GAA ATA CCT GGT ATT GGC-3′ for I261M, 5′-CCA AAT GTC TTA AAG CAC TGG GTA TCA ATA GTG TGC G-3′ for E276K, 5′-GTG AGA TTA ATA ATC CGT CGG AAT TCC TCT GAG AAG C-3′ for Y374N, and the corresponding antiparallel primer for each mutation. All four substitutions were confirmed by nucleotide sequence analyses of the constructed vectors.

Expression and Purification of Recombinant Proteins. The wild-type and variant forms of recombinant pol ι core proteins were expressed in *E. coli* strain BL21(DE3) cells. *E. coli* harboring each vector for the recombinant protein were grown in Luria−Bertani broth supplemented with kanamycin (50 μg mL^{-1}) at 37 °C, with aeration, to an OD_{600} of 0.6. Isopropyl-β-D-thiogalactopyranoside was added to 0.2 mM, and incubation was continued for 14 h at 16 °C. The cells were harvested by centrifugation and resuspended in lysis buffer (50 mM Tris-HCl, pH 7.4, containing 300 mM NaCl, 10% glycerol (v/v), 5 mM β-mercaptoethanol, 1 mg lysozyme mL^{-1}, and protease inhibitor cocktail), cooled on ice for 30 min, and then lysed by sonication (12 × 10 s duration with a Branson digital sonifier microtip, (VWR, West Chester, PA), 45% amplitude, with intermittent cooling time). The cell lysate was clarified by centrifugation at 4 × 10^4 × g for 60 min at 4 °C. The resulting supernatant was loaded onto a 1 mL GSTrap 4B column, and the column was washed with 20 mL of Buffer A (50 mM Tris-HCl, pH 7.4, containing 150 mM NaCl, 10% glycerol (v/v), and 5 mM β-mercaptoethanol). GST-tagged pol ι core bound on the column was cleaved by Prescission Protease for 14 h at 4 °C. Cleaved pol ι core fractions (eluted with Buffer A) were collected and diluted 6-fold with buffer B (50 mM Tris-HCl (pH 7.4), 1 mM EDTA, 10% glycerol (v/v), and 5 mM β-mercaptoethanol). Pol ι core was further purified to near homogeneity with the use of a Mono S column and a 50 mM to 2 M NaCl gradient in buffer B. Pol ι core was eluted at ∼250 mM NaCl. Protein concentrations were estimated using a Bradford protein assay, and the quality of purified proteins was assessed by SDS-polyacrylamide gel electrophoresis and Coomassie Brilliant Blue staining (Figure S1, Supporting Information).

DNA Polymerization Assays and Steady-State Kinetic Analysis. Standard DNA polymerase reactions of 8 μL were performed in 50 mM Tris-HCl (pH 7.5) buffer containing 50 mM

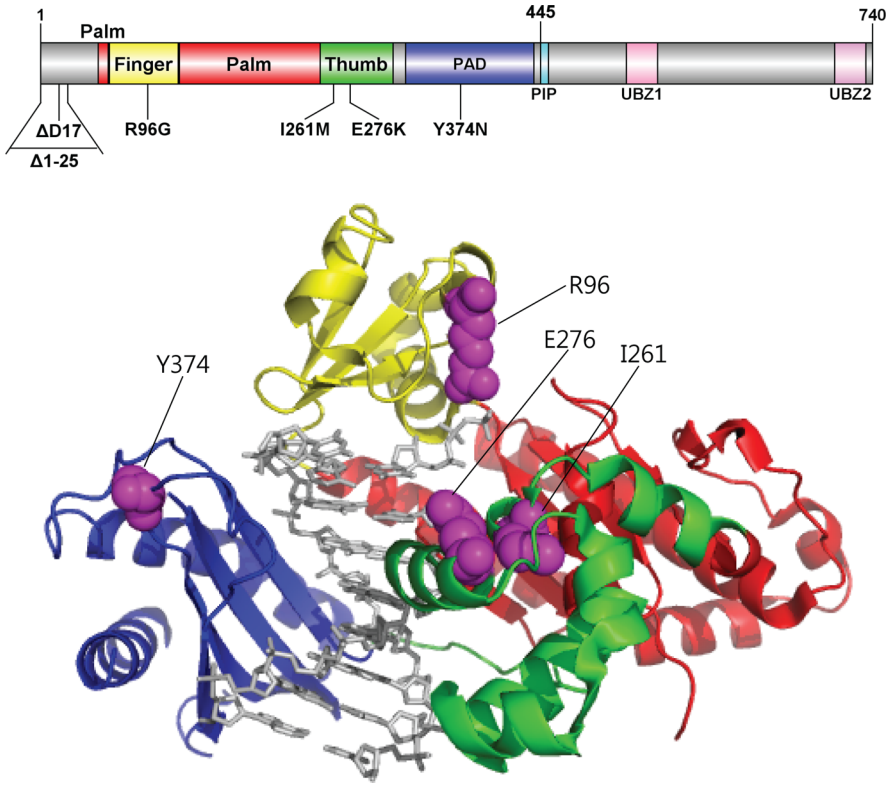

Figure 1. Locations of genetic pol ι variations. Structure of human pol ι(26−445) (PDB code, 2FLL) bound to primer/template DNA and incoming nucleotide is shown using Pymol. Pol ι(26−445) is shown in cartoon ribbons, and the primer/template DNA and nucleotide are shown in gray sticks. The finger, palm, thumb, and PAD domains are colored yellow, red, green, and blue, respectively. The amino acid residues (in purple spheres) of genetic pol ι variants are indicated. The structural domains of pol ι are shown in the upper schematic diagram using DOG (version 2.0),[60] where positions of amino acids related to six studied variations are indicated.

NaCl, 5 mM dithiothreitol, 100 μg mL^{-1} bovine serum albumin (BSA) (w/v), and 10% glycerol (v/v) with 100 nM primer-template substrate at 37 °C. Reactions were initiated by the addition of dNTPs with $MgCl_2$ (5 mM final concentration) or $MnCl_2$ (0.15 mM final concentration) to preincubated enzyme/DNA mixtures and terminated with six volumes of a solution of 20 mM EDTA in 95% formamide (v/v). For steady-state kinetic analysis, the primer-template was extended in the presence of 0.1−33 nM pol ι enzyme (or up to 400 nM enzyme for R96G) with increasing concentrations of individual dNTPs for 10 min, when the maximum amount of extension products was ≤20% of total DNA substrates. Products were resolved using a 16% polyacrylamide (w/v) gel electrophoresis system containing 8 M urea and visualized using a Bio-Rad Personal Molecular Imager and Quantity One software (Bio-Rad). The product formation rates (as a function of dNTP concentration) were plotted to estimate the kinetic parameters K_m and k_{cat} by nonlinear regression fitting to the Michaelis−Menten equation using Graph Pad Prism 5.0 software (GraphPad, San Diego, CA). Misinsertion frequency (f_{ins}) opposite G or G adducts was calculated as $f_{ins} = (k_{cat}/K_m)_{dNTP}/(k_{cat}/K_m)_{dCTP}$.[34]

Fluorescence Polarization Experiments. The 2 nM 18-FAM-mer primer annealed with unmodified 36-mer template was incubated with varying concentrations of pol ι, and fluorescence polarization (FP) was measured with a Biotek Synergy NEO plate reader (Winooski, VT) using excitation and emission wavelengths of 485 and 528 nm, respectively. The polymerase-DNA binding reaction was done in the presence of 50 mM HEPES buffer (pH 7.5) containing 10 mM potassium acetate, 10 mM KCl, 0.1 mM EDTA, 2 mM β-mercaptoethanol, and 0.1 mg mL^{-1} BSA in the presence of $MgCl_2$ or $MnCl_2$ (final 0.15 or 1 mM concentration), as modified from a previous study.[35] FP data were plotted vs enzyme concentration and fit to a quadratic equation to estimate $K_{d,DNA}$ using the equation: $P = P_0 + (P_{max} - P_0)((D_t + E_t + K_{d,DNA}) - ((D_t + E_t + K_{d,DNA})^2 - (4D_tE_t))^{1/2})/(2D_t)$, where P is the measured change in polarization (in units of millipolarization (mP)), P_0 is initial polarization (DNA alone), P_{max} is maximum polarization, D_t is DNA concentration, E_t is enzyme concentration, and $K_{d,DNA}$ is the equilibrium dissociation constant for enzyme binding to DNA.

RESULTS

Overall Study Approach. The aim of this study was to analyze the potentially dysfunctional germ-line genetic variants of human pol ι and identify functional pol ι variants. To achieve this, we first screened for human *POLI* genetic variations likely to alter the enzymatic function of pol ι from the dbSNP database. We utilized the new annotated open reading frame (ORF) sequence of the *POLI* gene as described in GenBank accession number NM_007195 (http://www.ncbi.nlm.nih.gov/genbank/), which encodes a pol ι protein of 740 amino acids with an additional 25 amino acids at the *N*-terminus compared to the previous wild-type, in that the previous ORF of pol ι was erroneously annotated to start at a site 75 bases downstream of the actual translational initiation site.[36] We picked four candidate variations by searching for non-synonymous coding variations that are located in the polymerase core domains (finger, palm, thumb, and little finger) and are also predicted as damaging with prediction tools (SIFT and PolyPhen). The SIFT algorithm utilizes a sequence homology-based approach to classify amino acid substitutions, which is based on the evolutionary conservation of the amino acids within protein families,[30] while the PolyPhen algorithm uses both sequence- and structure-based prediction.[31,32] The R96G variation (close to the incoming nucleotide at the finger

dx.doi.org/10.1021/tx5002755 | Chem. Res. Toxicol. 2014, 27, 1837−1852

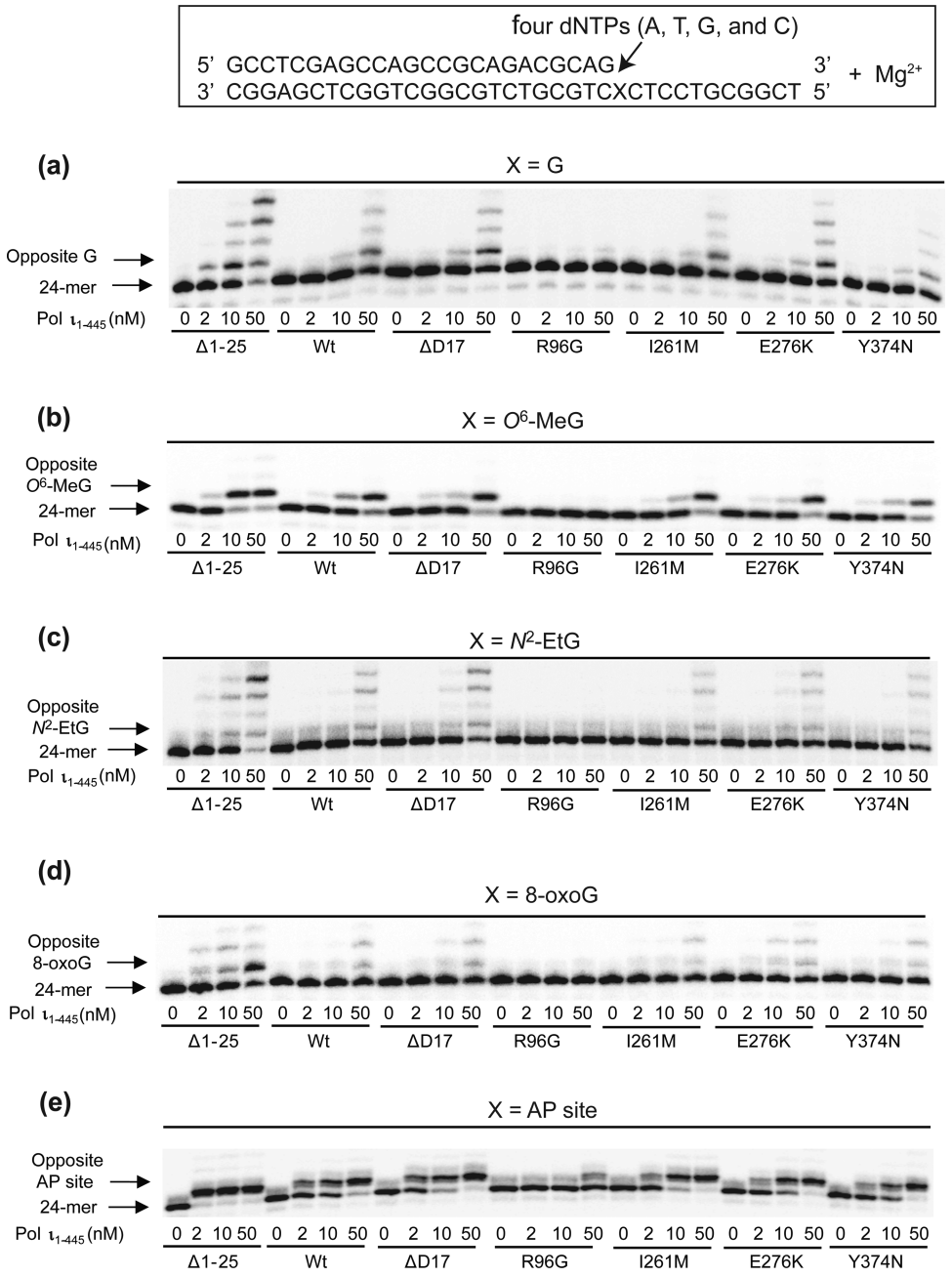

Figure 2. Extension of ^{32}P-labeled primers opposite G, O^6-MeG, N^2-EtG, 8-oxoG, and an abasic site by human wild-type pol ι (1−445) and variants in the presence of Mg^{2+}. The primer (24-mer) was annealed with each of the five different 36-mer templates containing an unmodified G, O^6-MeG, N^2-EtG, 8-oxoG, or abasic site placed at the 25th position from the 3′-end. Reactions were done in the presence of 5 mM $MgCl_2$ for 15 min with DNA substrate (100 nM primer/template), all four dNTPs (50 μM each), and increasing concentrations of pol ι (0−50 nM) as indicated. The extension products were separated by denaturing gel electrophoresis and imaged using a phosphorimager.

domain) and the I261M and E276K variations (in the thumb domain) were predicted to be damaging by both SIFT and PolyPhen, while the Y374N variation in the little finger domain was predicted to be damaging only by SIFT (Table 1 and Figure 1). We also selected two more candidate variations that would result in an altered translation initiation or an amino acid deletion at the N-terminal extension of 25 amino acids (Table 1 and Figure 1), one of which is the initiator codon variation (c.3G > A) to mutate the start codon (ATG) to a nonstart codon (ATA) and thus theoretically yield the variant protein deleted of the first 25 *N*-terminal residues (Δ1−25) that was previously referred to the wild-type enzyme. After that, we investigated the biochemical impact of six genetic variations on the enzymatic features of pol ι in both normal and translesion DNA synthesis at G and various DNA lesions. To effectively observe the alterations of polymerase function in six selected pol ι variants of the polymerase core domains, we utilized the core protein (amino acids 1−445) of pol ι, which contains all the polymerase core domains critical to polymerase activity. The previous core protein (26−445) was also shown to have the similar polymerase activity to the previous full-length pol ι (26−740).[37] A set of experiments, including "standing-start" full-length primer extensions, steady-state kinetics of nucleotide incorporation opposite the lesions, and pol ι-DNA binding

dx.doi.org/10.1021/tx5002755 | *Chem. Res. Toxicol.* 2014, 27, 1837−1852

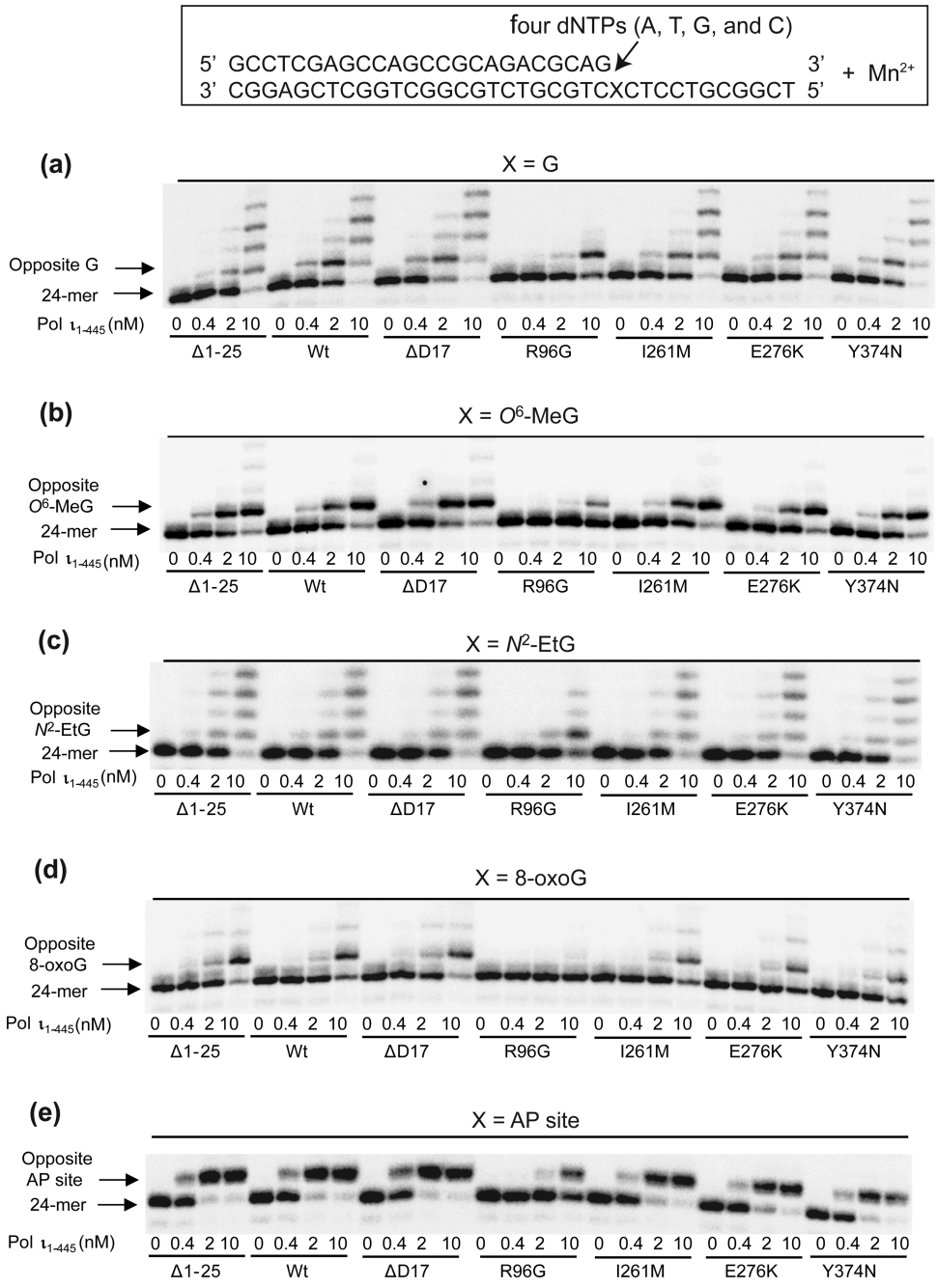

Figure 3. Extension of ^{32}P-labeled primers opposite G, O^6-MeG, N^2-EtG, 8-oxoG, and an abasic site by human wild-type pol ι (1−445) and variants in the presence of Mn^{2+}. Primer (24-mer) was annealed with each of the five different 36-mer templates containing an unmodified G, O^6-MeG, N^2-EtG, 8-oxoG, or abasic site placed at the 25th position from the 3′-end. Reactions were done in the presence of 0.15 mM $MnCl_2$ for 15 min with DNA substrate (100 nM primer/template), all four dNTPs (50 μM each), and increasing concentrations of pol ι (0−10 nM) as indicated. The extension products were separated by denaturing gel electrophoresis and imaged using a phosphorimager.

assays, was carried out successively using the recombinant core (1−445 amino acids) of pol ι enzymes and oligonucleotides containing a normal G or each of four bypassable DNA lesions, i.e., N^2-EtG, O^6-MeG, 8-oxoG, or abasic site at a defined site. We also compared the effects of two metals—Mn^{2+} and Mg^{2+}—in these experiments because pol ι is known to prefer Mn^{2+} to Mg^{2+} in polymerase catalysis.[20]

Primer Extension across G and DNA Lesions with All Four dNTPs by Wild-Type and Variant Pol ι Enzymes in the Presence of $MgCl_2$. To evaluate the possible changes in Mg^{2+}-dependent DNA polymerase activities of six human pol ι variants at undamaged and damaged DNA templates, we performed "standing-start" primer extensions with the wild-type and variant pol ι proteins using 24-mer/36-mer duplexes containing a G, N^2-EtG, O^6-MeG, 8-oxoG, or abasic site at position 25 of the template in the presence of all four dNTPs and 5 mM $MgCl_2$ (Figure 2). Those four DNA adducts, which were previously found to be bypassed relatively efficiently by human pol ι,[11,17,19,38] were selected as the favored substrate lesions of pol ι. Wild-type pol ι extended about half of the primers past G and yielded mainly one-base extended 25-mer products with some traces of 26- and 27-mers (with a 50 nM

dx.doi.org/10.1021/tx5002755 | Chem. Res. Toxicol. 2014, 27, 1837−1852

Table 2. Steady-State Kinetic Parameters for dNTP Incorporation Opposite G, O^6-MeG, and N^2-EtG by Wild-Type and Variant hPols ι(1-445) in the Presence of 5 mM Mg^{2+}

template	pol ι(1−445)	dNTP	K_m (μM)	k_{cat} (s^{-1})	k_{cat}/K_m (s^{-1} mM^{-1})	f_{ins}[a]	relative efficiency[b]
G	wild-type	C	1100 ± 300	0.021 ± 0.002	0.019	1	1
		T	1800 ± 400	0.0093 ± 0.0007	0.0052	0.27	
	Δ1−25	C	370 ± 47	0.042 ± 0.002	0.11	1	5.8
		T	1000 ± 100	0.037 ± 0.002	0.037	0.34	
	ΔD17	C	1900 ± 300	0.046 ± 0.002	0.024	1	1.3
		T	2900 ± 1000	0.013 ± 0.002	0.0045	0.19	
	R96G	C	3100 ± 800	0.0015 ± 0.0001	0.00048	1	0.025
		T	820 ± 230[c]	0.00015 ± 0.00001	0.00018	0.38	
	I261M	C	1500 ± 100	0.034 ± 0.0008	0.023	1	1.2
		T	2400 ± 600	0.0078 ± 0.0007	0.0033	0.14	
	E276K	C	1700 ± 200	0.03 ± 0.001	0.018	1	0.95
		T	4700 ± 1600	0.014 ± 0.002	0.0030	0.17	
	Y374N	C	1900 ± 200	0.022 ± 0.001	0.012	1	0.63
		T	3400 ± 900	0.0079 ± 0.0008	0.0023	0.19	
O^6-MeG	wild-type	C	1800 ± 500	0.033 ± 0.004	0.018	1	1
		T	940 ± 170	0.027 ± 0.002	0.029	1.6	
	Δ1−25	C	620 ± 180	0.10 ± 0.01	0.16	1	8.9
		T	170 ± 50	0.043 ± 0.003	0.25	1.6	
	ΔD17	C	2800 ± 600	0.055 ± 0.005	0.020	1	1.1
		T	1400 ± 300	0.088 ± 0.006	0.063	3.2	
	R96G	C	3000 ± 800	0.0011 ± 0.0001	0.00036	1	0.02
		T	3200 ± 600	0.0010 ± 0.0001	0.00032	0.89	
	I261M	C	2200 ± 800	0.034 ± 0.004	0.018	1	1.0
		T	1100 ± 200	0.039 ± 0.002	0.035	1.9	
	E276K	C	1800 ± 400	0.029 ± 0.002	0.016	1	0.89
		T	1600 ± 300	0.042 ± 0.003	0.026	1.6	
	Y374N	C	2200 ± 500	0.048 ± 0.005	0.022	1	1.2
		T	1500 ± 400	0.043 ± 0.004	0.029	1.3	
N^2-EtG	wild-type	C	2800 ± 400	0.018 ± 0.001	0.0064	1	1
		T	2700 ± 200	0.012 ± 0.0003	0.0044	0.69	
	Δ1−25	C	550 ± 60	0.048 ± 0.001	0.087	1	14
		T	770 ± 110	0.033 ± 0.001	0.043	0.49	
	ΔD17	C	3000 ± 300	0.028 ± 0.0001	0.0093	1	1.5
		T	2800 ± 200	0.020 ± 0.001	0.0071	0.76	
	R96G	C	5400 ± 1600	0.0040 ± 0.0005	0.00074	1	0.12
		T	1600 ± 100	0.00049 ± 0.00009	0.00031	0.41	
	I261M	C	2000 ± 300	0.015 ± 0.001	0.0075	1	1.2
		T	1900 ± 700	0.012 ± 0.002	0.0063	0.84	
	E276K	C	3700 ± 500	0.026 ± 0.002	0.0070	1	1.1
		T	3700 ± 400	0.021 ± 0.001	0.0057	0.81	
	Y374N	C	1400 ± 200	0.017 ± 0.001	0.012	1	1.9
		T	2100 ± 700	0.013 ± 0.002	0.0062	0.52	

[a]Misinsertion frequency, calculated by dividing k_{cat}/K_m for dNTP incorporation by the k_{cat}/K_m for dCTP incorporation opposite template base. All values are presented to two significant digits. [b]Relative efficiency, calculated by dividing k_{cat}/K_m of each pol ι(1−445) for dCTP incorporation opposite template base by k_{cat}/K_m of wild-type pol ι(1−445) for dCTP incorporation opposite template base. [c]The apparent K_m value, determined under the condition where the amount of enzyme is greater than the amount of DNA and thus is not strictly steady-state.

enzyme concentration), and this pattern was also observed with the ΔD17, I261M, E276K, and Y374N variants. However, the Δ1−25 variant readily synthesized products mainly up to 27- and 28-mers and seemed much more effective than the wild-type enzyme. In contrast, the R96G variant generated almost no extension at G even with a 50 nM enzyme concentration, indicating severe impairment of polymerase activity due to this amino acid substitution. For translesion synthesis at N^2-EtG, O^6-MeG, 8-oxoG, or an abasic lesion, those six variants showed a similar trend of results as that observed with an undamaged G template, although the extents of bypass synthesis across each lesions differed from one another. With each of those four lesions, the Δ1−25 variant yielded considerably more one-base or up to four-base extended products than the wild-type, while the R96G variant yielded only a trace of one-base or almost no extension at the lesions. Similar patterns were also observed in the presence of 1 mM $MgCl_2$ (at which pol ι was observed to be maximally active with normal DNA substrates tested, results not shown). These results indicate that R96G and Δ1−25 pol ι variants might have a defective and hyperactive Mg^{2+}-dependent TLS ability, respectively.

Primer Extension across G and DNA Lesions with All Four dNTPs by Wild-Type and Variant Pol ι Enzymes in the Presence of $MnCl_2$. To examine the effect of Mn^{2+} as a

dx.doi.org/10.1021/tx5002755 | Chem. Res. Toxicol. 2014, 27, 1837−1852

Table 3. Steady-State Kinetic Parameters for dNTP Incorporation Opposite 8-oxoG by Wild-Type and Variant hPols ι(1-445) in the Presence of 5 mM Mg^{2+}

pol ι(1−445)	dNTP	K_m (μM)	k_{cat} (s^{-1})	k_{cat}/K_m (s^{-1} mM^{-1})	f_{ins}[a]	relative efficiency[b]
wild-type	A	1300 ± 200	0.00081 ± 0.00005	0.00062	0.077	
	T	1600 ± 300	0.0027 ± 0.0002	0.0017	0.27	
	G	230 ± 40	0.0032 ± 0.0001	0.014	1.7	
	C	1600 ± 300	0.013 ± 0.001	0.0081	1	1
Δ1−25	A	530 ± 80	0.0034 ± 0.00017	0.0064	0.13	
	T	510 ± 70	0.0074 ± 0.0003	0.015	0.31	
	G	120 ± 10	0.0061 ± 0.00014	0.051	1.1	
	C	1200 ± 100	0.057 ± 0.002	0.048	1	5.9
ΔD17	A	1000 ± 200	0.00088 ± 0.00005	0.00088	0.14	
	T	2400 ± 200	0.0046 ± 0.0001	0.0019	0.30	
	G	530 ± 50	0.0062 ± 0.0002	0.012	1.9	
	C	4000 ± 900	0.025 ± 0.003	0.0063	1	0.78
R96G	A	840 ± 30[c]	0.000072 ± 0.000008	0.000086	0.36	
	T	290 ± 70	0.00018 ± 0.00001	0.00062	2.6	
	G	160 ± 20[c]	0.00010 ± 0.000003	0.00063	2.6	
	C	1900 ± 400	0.00045 ± 0.00004	0.00024	1	0.030
I261M	A	820 ± 110	0.00075 ± 0.00003	0.00092	0.21	
	T	1400 ± 300	0.0028 ± 0.0002	0.0020	0.47	
	G	320 ± 20	0.0044 ± 0.0001	0.014	3.3	
	C	2100 ± 300	0.0090 ± 0.0005	0.0043	1	0.53
E276K	A	1500 ± 100	0.0010 ± 0.00002	0.00066	0.11	
	T	2200 ± 200	0.0055 ± 0.0002	0.0025	0.43	
	G	920 ± 30	0.012 ± 0.0001	0.013	2.2	
	C	3800 ± 200	0.022 ± 0.001	0.0058	1	0.72
Y374N	A	1000 ± 100	0.00061 ± 0.00003	0.00061	0.086	
	T	1200 ± 200	0.0023 ± 0.0001	0.0019	0.27	
	G	260 ± 20	0.0030 ± 0.0001	0.013	1.8	
	C	1700 ± 800	0.012 ± 0.002	0.0071	1	0.88

[a]Misinsertion frequency, calculated by dividing k_{cat}/K_m for dNTP incorporation by the k_{cat}/K_m for dCTP incorporation opposite 8-oxoG. All values are presented to two significant digits. [b]Relative efficiency, calculated by dividing k_{cat}/K_m of each pol ι(1−445) for dCTP incorporation opposite 8-oxoG by k_{cat}/K_m of wild-type pol ι(1−445) for dCTP incorporation opposite 8-oxoG. [c]The apparent K_m value, determined under the condition where the amount of enzyme is greater than the amount of DNA and thus is not strictly steady-state.

prosthetic group (instead of Mg^{2+}) on normal and translesion polymerase activities by six variants, standing-start primer extension experiments were done with the wild-type and variant pol ι proteins using 24-mer primers annealed to 36-mer templates containing G, N^2-EtG, O^6-MeG, 8-oxoG, or an abasic site in the presence of all four dNTPs and 0.15 mM $MnCl_2$ (Figure 3). Wild-type pol ι extended most 24-mer primers across G and four lesions and yielded 25- or up to 28-mer products (10 nM enzyme concentration with 0.15 mM Mn^{2+}, Figure 3A), more effectively than with 5 mM Mg^{2+} (Figure 2A), indicating a catalytic preference of pol ι for Mn^{2+} compared to Mg^{2+}, as expected from the previous literature.[20] The primer extension results for each pol ι protein across G and four lesions in the presence of Mn^{2+} were almost similar to those with Mg^{2+} except for the case of the Δ1−25 variant. Opposite G and four DNA lesions, the R96G variant generated extension products considerably lower in extent than the wild-type in the presence of Mn^{2+} (Figure 3A), as similarly observed with Mg^{2+} (Figure 2A), although the decrease of R96G bypass extent was less opposite template N^2-EtG than the other templates. However, the Δ1−25 variant extended the primers across G and four lesions to a similar extent as the wild-type pol ι in the presence of Mn^{2+} (Figure 3), in contrast to the increase in Mg^{2+}-dependent polymerase activity of this variant (Figure 2).

Steady-State Kinetics of Nucleotide Incorporation Opposite DNA Lesions by the Wild-Type and Variant Pol ι Enzymes in the Presence of $MgCl_2$. To analyze the efficiency and fidelity of six pol ι variants for Mg^{2+}-dependent nucleotide insertion opposite G and four DNA lesions, we determined steady-state kinetic parameters for incorporation of single nucleotides into 24-mer/36-mer duplexes opposite a G or each of four lesions in the presence of 5 mM $MgCl_2$ by six variants in comparison to wild-type pol ι (Tables 2−4). The values of k_{cat}/K_m and misinsertion frequency ($f = (k_{cat}/K_m)_{incorrect\ dNTP}/(k_{cat}/K_m)_{correct\ dNTP}$) were employed as semi-quantitative measures for the nucleotide insertion efficiency and fidelity of a distributive pol ι, as applied in previous work.[19] Wild-type pol ι inserted single nucleotides opposite each template with the efficiency order (based on the maximum k_{cat}/K_m) abasic lesion > O^6-MeG > G > 8-oxoG > N^2-EtG. Wild-type pol ι inserted the correct dCTP in slight preference to dTTP opposite G and N^2-EtG but misinserted dTTP and dGTP (in preference to dCTP) opposite O^6-MeG and 8-oxoG, respectively, while inserting nucleoside triphosphates opposite an abasic site in the preferential order of dGTP > dTTP > dATP > dCTP. The ΔD17, I261M, E276K, and Y374N variants inserted dCTP in preference to dTTP opposite undamaged G, with the values of k_{cat}/K_m similar to those of wild-type pol ι. However, the R96G variant showed ∼40-fold reductions in k_{cat}/K_m values for dCTP and dTTP insertion opposite G compared to wild-type pol ι, while the Δ1−25 variant showed 6- to 7-fold increases in those values. Similar

dx.doi.org/10.1021/tx5002755 | Chem. Res. Toxicol. 2014, 27, 1837−1852

Table 4. Steady-State Kinetic Parameters for dNTP Incorporation Opposite Abasic Site by Wild-Type and Variant hPols ι(1-445) in the Presence of 5 mM Mg^{2+}

pol ι(1−445)	dNTP	K_m (μM)	k_{cat} (s^{-1})	k_{cat}/K_m (s^{-1} mM^{-1})	dNTP selectivity ratio[a]	relative efficiency[b]
wild-type	A	1100 ± 30	0.081 ± 0.007	0.074	0.46	
	T	600 ± 90	0.058 ± 0.002	0.097	0.61	
	G	770 ± 110	0.12 ± 0.01	0.16	1	1
	C	830 ± 550	0.027 ± 0.005	0.033	0.21	
Δ1−25	A	160 ± 10	0.15 ± 0.002	0.94	0.72	
	T	140 ± 20	0.18 ± 0.01	1.3	1	
	G	230 ± 50	0.21 ± 0.01	0.91	0.70	5.7
	C	680 ± 100	0.14 ± 0.01	0.21	0.16	
ΔD17	A	770 ± 200	0.081 ± 0.006	0.11	0.61	
	T	760 ± 50	0.10 ± 0.002	0.13	0.72	
	G	910 ± 90	0.17 ± 0.01	0.18	1	1.1
	C	2100 ± 800	0.074 ± 0.010	0.035	0.19	
R96G	A	1700 ± 500	0.0035 ± 0.0003	0.0021	0.26	
	T	820 ± 64	0.0066 ± 0.0002	0.0080	1	
	G	1600 ± 400	0.0048 ± 0.0008	0.0030	0.38	0.019
	C	1800 ± 400	0.0012 ± 0.0001	0.00067	0.084	
I261M	A	690 ± 60	0.053 ± 0.002	0.077	0.64	
	T	480 ± 90	0.051 ± 0.003	0.11	0.92	
	G	670 ± 80	0.080 ± 0.003	0.12	1	0.75
	C	860 ± 250	0.031 ± 0.002	0.036	0.30	
E276K	A	1400 ± 100	0.086 ± 0.004	0.064	0.49	
	T	1000 ± 100	0.079 ± 0.002	0.079	0.61	
	G	950 ± 110	0.13 ± 0.01	0.13	1	0.81
	C	2000 ± 300	0.054 ± 0.002	0.027	0.21	
Y374N	A	850 ± 210	0.047 ± 0.004	0.056	0.58	
	T	600 ± 90	0.056 ± 0.003	0.093	0.97	
	G	1000 ± 200	0.096 ± 0.007	0.096	1	0.60
	C	1200 ± 100	0.032 ± 0.003	0.027	0.28	

[a]dNTP selectivity ratio, calculated by dividing k_{cat}/K_m of each dNTP incorporation by the highest k_{cat}/K_m for dNTP incorporation opposite the abasic site. All values are presented to two significant digits. [b]Relative efficiency, calculated by dividing k_{cat}/K_m of each pol ι(1−445) for dGTP incorporation opposite the abasic site by k_{cat}/K_m of wild-type pol ι(1−445) for dGTP incorporation opposite the abasic site.

trends of results were observed with four DNA lesion templates, with some alterations in nucleotide preference for some cases. The R96G variant displayed about 8-, 33-, 50-, and 72-fold reductions in k_{cat}/K_m values for dCTP insertion, respectively, opposite N^2-EtG, 8-oxoG, O^6-MeG, and an abasic site compared to wild-type pol ι, with 5- and 10-fold increases in misinsertion frequencies for A and T opposite 8-oxoG but a 3-fold decrease in misinsertion frequency for T opposite O^6-MeG. However, the Δ1−25 variant displayed 6- to 14-fold increases in k_{cat}/K_m for correct dCTP insertion opposite four lesions compared to wild-type pol ι, with misinsertion frequencies similar to the wild-type protein. Interestingly, both the Δ1−25 and R96G variants slightly preferred dTTP over dGTP for insertion opposite an abasic site, as opposed to the case of the wild-type pol ι, which prefers to insert dGTP (Table 4).

Steady-State Kinetics of Nucleotide Incorporation Opposite DNA Lesions by the Wild-Type and Variant Pol ι Enzymes in the Presence of $MnCl_2$. To evaluate the efficiency and fidelity in Mn^{2+}-dependent nucleotide insertion opposite G and DNA lesions by six pol ι variants, we determined steady-state kinetic parameters for nucleotide incorporation opposite a G or each of four lesions in the presence of 0.15 mM $MnCl_2$ by six variants in comparison to the wild-type (Tables 5−7). The k_{cat}/K_m values of wild-type pol ι for Mn^{2+}-dependent dCTP and dTTP insertion opposite G were 3 orders of magnitude higher than those of the wild-type protein for Mg^{2+}-dependent insertion. For Mn^{2+}-dependent nucleotide insertion, most of the variants (including the Δ1−25 variant) showed the k_{cat}/K_m values similar to those of wild-type, whereas the R96G variant displayed 29- to 41-fold reduction in k_{cat}/K_m compared to wild-type (Table 5). Similar trends of results were observed with four DNA lesion templates, except for the case with the template N^2-EtG and the R96G variant. The R96G variant showed about 16-, 8-, and 5-fold decreases in k_{cat}/K_m values for dCTP insertion, respectively, opposite O^6-MeG, 8-oxoG, and the abasic site compared to those of the wild-type protein, while showing a 9-fold increase in activity opposite N^2-EtG compared to wild-type, indicating that the R96G variation might substantially impair Mn^{2+}-dependent TLS opposite O^6-MeG, 8-oxoG, and an abasic site but facilitate that only opposite N^2-EtG. These steady-state kinetic data might in large part explain the relatively proficient Mn^{2+}-dependent bypass of the R96G variant opposite N^2-EtG compared to the other lesions (Figure 3).

Binding of the Wild-Type Pol ι(1−445) and the Variants Δ1−25 and R96G to DNA Substrate. To analyze the binding affinities of two dysfunctional pol ι variants, Δ1−25 and R96G, for the primer-template DNA substrate in the presence of either Mg^{2+} or Mn^{2+}, we performed fluorescence polarization experiments. The equilibrium dissociation constants ($K_{d,DNA}$) of wild-type pol ι and the Δ1−25 and R96G variants were estimated by fitting the fluorescence polarization values of fluorescein-labeled DNA substrates (18-FAM-mer

dx.doi.org/10.1021/tx5002755 | Chem. Res. Toxicol. 2014, 27, 1837−1852

Table 5. Steady-State Kinetic Parameters for dNTP Incorporation Opposite G, O^6-MeG, and N^2-EtG by Wild-Type and Variant hPols ι(1-445) in the Presence of 0.15 mM Mn^{2+}

template	pol ι(1−445)	dNTP	K_m (μM)	k_{cat} (s^{-1})	k_{cat}/K_m (s^{-1} mM^{-1})	f_{ins}[a]	relative efficiency[b]
G	wild-type	C	1.5 ± 0.1	0.11 ± 0.002	73	1	1
		T	3.3 ± 0.2	0.094 ± 0.002	28	0.38	
	Δ1−25	C	0.52 ± 0.05	0.036 ± 0.0007	72	1	0.99
		T	1.2 ± 0.1	0.055 ± 0.001	46	0.64	
	ΔD17	C	1.4 ± 0.003	0.12 ± 0.003	86	1	1.2
		T	3.6 ± 0.2	0.12 ± 0.002	33	0.38	
	R96G	C	11 ± 1	0.028 ± 0.001	2.5	1	0.034
		T	11 ± 1	0.0075 ± 0.0003	0.68	0.27	
	I261M	C	1.3 ± 0.08	0.068 ± 0.0009	52	1	0.71
		T	3.0 ± 0.2	0.068 ± 0.001	23	0.44	
	E276K	C	1.4 ± 0.08	0.051 ± 0.0006	36	1	0.49
		T	3.4 ± 0.1	0.047 ± 0.0005	14	0.39	
	Y374N	C	2.6 ± 0.2	0.14 ± 0.003	54	1	0.74
		T	3.8 ± 0.2	0.095 ± 0.001	25	0.46	
O^6-MeG	wild-type	C	3.9 ± 0.1	0.10 ± 0.001	26	1	1
		T	3.2 ± 0.2	0.069 ± 0.001	22	0.85	
	Δ1−25	C	1.6 ± 0.09	0.039 ± 0.0005	24	1	0.93
		T	1.4 ± 0.2	0.027 ± 0.001	19	0.79	
	ΔD17	C	3.8 ± 0.2	0.18 ± 0.003	47	1	1.8
		T	2.5 ± 0.4	0.087 ± 0.003	35	0.74	
	R96G	C	12 ± 3	0.019 ± 0.002	1.6	1	0.062
		T	4.3 ± 0.6	0.0073 ± 0.0003	1.7	1.1	
	I261M	C	2.3 ± 0.1	0.075 ± 0.001	33	1	1.3
		T	4.0 ± 0.5	0.036 ± 0.001	9.0	0.27	
	E276K	C	2.5 ± 0.1	0.044 ± 0.0006	18	1	0.69
		T	3.2 ± 0.4	0.038 ± 0.001	12	0.67	
	Y374N	C	3.7 ± 0.3	0.077 ± 0.001	21	1	0.81
		T	2.0 ± 0.3	0.050 ± 0.002	25	1.2	
N^2-EtG	wild-type	C	27 ± 2	0.034 ± 0.001	1.3	1	1
		T	80 ± 5	0.045 ± 0.001	0.56	0.44	
	Δ1−25	C	7.5 ± 1.1	0.011 ± 0.001	1.5	1	1.2
		T	29 ± 2	0.018 ± 0.0005	0.62	0.42	
	ΔD17	C	13 ± 1	0.025 ± 0.001	1.9	1	1.5
		T	93 ± 12	0.044 ± 0.003	0.47	0.24	
	R96G	C	3.7 ± 0.1	0.045 ± 0.0004	12	1	9.2
		T	26 ± 9	0.0058 ± 0.0008	0.22	0.018	
	I261M	C	16 ± 2	0.023 ± 0.001	1.4	1	1.1
		T	87 ± 11	0.042 ± 0.002	0.48	0.34	
	E276K	C	20 ± 5	0.018 ± 0.002	0.90	1	0.69
		T	92 ± 13	0.042 ± 0.003	0.46	0.51	
	Y374N	C	33 ± 3	0.039 ± 0.02	1.2	1	0.92
		T	82 ± 4	0.035 ± 0.001	0.43	0.36	

[a]Misinsertion frequency, calculated by dividing k_{cat}/K_m for each dNTP incorporation by the k_{cat}/K_m for dCTP incorporation opposite template base. All values are presented to two significant digits. [b]Relative efficiency, calculated by dividing k_{cat}/K_m of each pol ι(1−445) for dCTP incorporation opposite template base by k_{cat}/K_m of wild-type pol ι(1−445) for dCTP incorporation opposite template base.

primers annealed to unmodified 36-G-mer templates) as a function of the pol ι concentration to a quadratic equation (Table 8). Wild-type pol ι bound weakly to DNA with a $K_{d,DNA}$ of 490 and 840 nM, respectively, at 0.15 and 1 mM Mg^{2+}concentrations, while binding relatively tightly to DNA with a $K_{d,DNA}$ of 68 nM at 0.15 mM Mn^{2+} (but not at 1 mM Mn^{2+}). The R96G variant had $K_{d,DNA}$ values 2- to 3-fold higher than wild-type in the presence of either metal, indicating a slight decrease in DNA binding affinity of pol ι by this variant. In contrast, the Δ1−25 variant bound DNA much more tightly (20- to 29-fold) than the wild-type protein in the presence of 0.15 or 1 mM Mg^{2+}. Similarly, the Δ1−25 variant also had a DNA-binding affinity ($K_{d,DNA}$ = 140 nM) ∼10-fold lower than that of wild-type in the presence of 5 mM Mg^{2+} (results not shown). This large difference in the DNA-binding affinities was reduced to only 4-fold in the presence of 0.15 mM of Mn^{2+}. These data indicate that the N-terminal region (residues 1−25), rich in negatively charged amino acids, might severely interfere with DNA substrate binding of wild-type pol ι, but this interference could be totally ablated by the deletion of *N*-terminal 25 amino acids or could be substantially overcome by the low level of Mn^{2+}. These features might at least in part explain the substantial increase in polymerase activity of the Δ1−25 variant versus the wild-type pol ι seen in the presence of Mg^{2+} (Figure 2, Tables 2−4) but not with Mn^{2+} (Figure 3, Tables 5−7). Here we also note that the $K_{d,DNA}$ value (68 nM)

dx.doi.org/10.1021/tx5002755 | Chem. Res. Toxicol. 2014, 27, 1837−1852

Table 6. Steady-State Kinetic Parameters for dNTP Incorporation Opposite 8-oxoG by Wild-Type and Variant hPols ι(1-445) in the Presence of 0.15 mM Mn^{2+}

pol ι(1−445)	dNTP	K_m (μM)	k_{cat} (s^{-1})	k_{cat}/K_m (s^{-1} mM^{-1})	f_{ins}[a]	relative efficiency[b]
wild-type	A	2.0 ± 0.3	0.015 ± 0.001	7.5	0.83	
	T	30 ± 2	0.046 ± 0.002	1.5	0.17	
	G	0.90 ± 0.07	0.014 ± 0.0002	16	1.8	
	C	4.2 ± 0.2	0.038 ± 0.001	9.0	1	1
Δ1−25	A	17 ± 1	0.021 ± 0.0003	1.2	0.092	
	T	5.2 ± 0.3	0.028 ± 0.001	5.4	0.42	
	G	0.21 ± 0.1	0.0082 ± 0.0004	39	3.0	
	C	1.8 ± 0.2	0.023 ± 0.001	13	1	1.4
ΔD17	A	2.0 ± 0.2	0.017 ± 0.0003	8.5	0.77	
	T	29 ± 1	0.055 ± 0.001	5.3	0.48	
	G	0.53 ± 0.06	0.013 ± 0.0003	25	2.3	
	C	3.5 ± 0.2	0.040 ± 0.0006	11	1	1.2
R96G	A	3.3 ± 0.3	0.0017 ± 0.00004	0.52	0.43	
	T	13 ± 1	0.0046 ± 0.0001	0.35	0.29	
	G	1.8 ± 0.2	0.0038 ± 0.0001	2.1	1.8	
	C	8.5 ± 0.5	0.010 ± 0.0002	1.2	1	0.13
I261M	A	1.4 ± 0.2	0.015 ± 0.0004	11	1.0	
	T	25 ± 3	0.026 ± 0.001	1.0	0.091	
	G	0.66 ± 0.07	0.012 ± 0.0003	18	1.6	
	C	3.1 ± 0.1	0.034 ± 1.0003	11	1	1.2
E276K	A	2.2 ± 0.3	0.022 ± 0.001	10	1.4	
	T	24 ± 4	0.044 ± 0.003	1.8	0.26	
	G	0.60 ± 0.04	0.016 ± 0.0002	27	3.9	
	C	3.2 ± 0.2	0.022 ± 0.0004	6.9	1	0.77
Y374N	A	1.4 ± 0.1	0.015 ± 0.0003	11	1.0	
	T	29 ± 6	0.025 ± 0.003	0.86	0.078	
	G	0.72 ± 0.06	0.018 ± 0.0003	25	2.3	
	C	3.6 ± 0.1	0.040 ± 0.0003	11	1	1.2

[a]Misinsertion frequency, calculated by dividing k_{cat}/K_m for each dNTP incorporation by the k_{cat}/K_m for dCTP incorporation opposite 8-oxoG. All values are presented to two significant digits. [b]Relative efficiency, calculated by dividing k_{cat}/K_m of each pol ι(1−445) for dCTP incorporation opposite 8-oxoG by k_{cat}/K_m of wild-type pol ι(1−445) for dCTP incorporation opposite 8-oxoG.

of wild-type pol ι with Mn^{2+} would yield a relatively high dissociation rate, k_{off} (~0.68 s^{-1}), which might make pol ι very distributive.

DISCUSSION

In this study we examined the biochemical properties of six nonsynonymous coding variants of human pol ι in comparison with the wild-type, based on the newly annotated ORF sequence information. Four missense and two deletion variations were selected for this study because they were expected to cause functional alterations on pol ι on the basis of the nature of the changes, positions in the pol ι catalytic core, and predicted effects. Our biochemical data revealed that the R96G variation severely impairs the efficiency of pol ι for both normal and translesion syntheses at G, N^2-EtG, 8-oxoG, O^6-MeG, and an abasic site regardless of the presence of Mn^{2+} or Mg^{2+} (except for the case of a Mn^{2+}-facilitated C insertion opposite N^2-EtG), whereas the Δ1−25 deletion variation, which is equivalent to the previously misannotated wild-type, considerably increases pol ι efficiency for both normal and translesion syntheses in the presence of Mg^{2+} (but not with Mn^{2+}). The Δ1−25 variation greatly (20- to 29-fold) increased the DNA-binding affinity of pol ι in the presence of Mg^{2+}, which was much less prominent (only about ~4-fold) in the presence of a low concentration of Mn^{2+}. We also note that the poor DNA-binding affinity of the wild-type pol ι was considerably improved by the addition of a low level of Mn^{2+} when compared to that of Mg^{2+}. In this study we report that two rare, nonsynonymous *POLI* genetic variations can affect the TLS activities of human pol ι in opposite directions *in vitro* and that wild-type pol ι is substantially more sluggish in activity than expected from analysis of the previous wild-type protein (Δ1−25) in the presence of Mg^{2+}, unlike in the presence of Mn^{2+}.

To the best of our knowledge, this is the first study analyzing biochemical alterations in germline genetic variants and the newly denoted wild-type version of human pol ι, using *in vitro* polymerase activity, enzyme kinetics, and binding assays. Two of the six *POLI* genetic variations studied here were found to significantly affect the *in vitro* enzymatic function of pol ι in translesion DNA synthesis and DNA substrate binding. These functional genetic variations of pol ι appear to be rare, similar to dysfunctional pol κ variants we reported recently,[35] in that minor allele frequencies (MAFs) of the Δ1−25 and R96G pol ι variations are ~0.1% and 0.6%, respectively, in public databases (Table 1). The biological significance of rare frequency genetic variations should not be overlooked in that recent reports suggest the possible relevance of rare genetic variations to complex human diseases. Rare genetic variations have been proposed as a potential source of missing disease heritability that has not been fully explained by common genetic variations,[39] and the recent experimental reports support this view by providing evidence that rare genetic variations are abundantly present in human populations and are more likely

Table 7. Steady-State Kinetic Parameters for dNTP Incorporation Opposite Abasic Site by Wild-Type and Variant hPols ι(1-445) in the Presence of 0.15 mM Mn^{2+}

pol ι(1−445)	dNTP	K_m (μM)	k_{cat} (s^{-1})	k_{cat}/K_m (s^{-1} mM^{-1})	dNTP selectivity ratio[a]	relative efficiency[b]
wild-type	A	0.68 ± 0.04	0.012 ± 0.0001	18	0.18	
	T	1.5 ± 0.1	0.064 ± 0.001	43	0.43	
	G	0.29 ± 0.06	0.029 ± 0.001	100	1	1
	C	2.8 ± 0.1	0.066 ± 0.001	24	0.24	
Δ1−25	A	0.50 ± 0.06	0.010 ± 0.003	20	0.22	
	T	1.1 ± 0.1	0.024 ± 0.001	22	0.24	
	G	0.099 ± 0.005	0.0091 ± 0.0001	92	1	0.92
	C	0.98 ± 0.08	0.043 ± 0.001	44	0.48	
ΔD17	A	0.83 ± 0.13	0.016 ± 0.001	19	0.31	
	T	1.8 ± 0.2	0.048 ± 0.001	27	0.44	
	G	0.34 ± 0.04	0.021 ± 0.0004	62	1	0.62
	C	1.8 ± 0.3	0.11 ± 0.004	61	0.98	
R96G	A	1.9 ± 0.3	0.011 ± 0.0004	5.8	0.76	
	T	1.9 ± 0.2	0.0088 ± 0.0002	4.6	0.61	
	G	0.49 ± 0.06	0.0037 ± 0.0001	7.6	1	0.076
	C	3.4 ± 0.3	0.015 ± 0.0004	4.4	0.58	
I261M	A	0.35 ± 0.05	0.021 ± 0.001	60	0.50	
	T	1.3 ± 0.09	0.026 ± 0.0004	20	0.17	
	G	0.27 ± 0.02	0.032 ± 0.001	120	1	1.2
	C	2.5 ± 0.4	0.050 ± 0.002	20	0.17	
E276K	A	0.72 ± 0.11	0.017 ± 0.001	24	0.39	
	T	2.7 ± 0.3	0.028 ± 0.0007	10	0.16	
	G	0.34 ± 0.02	0.021 ± 0.0002	62	1	0.62
	C	2.2 ± 0.1	0.041 ± 0.0005	19	0.31	
Y374N	A	0.71 ± 0.09	0.026 ± 0.001	37	0.38	
	T	2.0 ± 0.2	0.082 ± 0.002	41	0.42	
	G	0.39 ± 0.03	0.038 ± 0.001	97	1	0.97
	C	3.3 ± 0.3	0.047 ± 0.001	14	0.14	

[a]dNTP selectivity ratio, calculated by dividing k_{cat}/K_m for each dNTP incorporation by the highest k_{cat}/K_m for dNTP incorporation opposite the abasic site. All values are presented to two significant digits. [b]Relative efficiency, calculated by dividing k_{cat}/K_m of each pol ι(1−445) for dGTP incorporation opposite the abasic site by k_{cat}/K_m of wild-type pol ι(1−445) for dGTP incorporation opposite the abasic site.

Table 8. K_d Values of Wild-Type hPol ι (1-445), and the Δ1−25 and R96G Variants for 18-FAM-mer/36-G-mer DNA Substrate in the Presence of $MnCl_2$ or $MgCl_2$

	K_d (nM) of pol ι(1−445)		
$MnCl_2$ or $MgCl_2$	wild-type	Δ1−25	R96G
0.15 mM $MnCl_2$	68 ± 11	17 ± 3	220 ± 50
0.15 mM $MgCl_2$	490 ± 70	17 ± 3	900 ± 200
1 mM $MnCl_2$	840 ± 250	88 ± 16	1800 ± 400
1 mM $MgCl_2$	840 ± 320	41 ± 7	1800 ± 600

to be misfunctional than common variations.[40,41] Only 19 nonsynonymous germline variations were described in 2008 (including two reported cancer-related SNPs[28,29]), but now a total of 91 nonsynonymous germline variations have been listed in dbSNP, most of which seem to be rare in that MAFs of 89 variations are either <1% or unavailable yet. About 46 types of missense and nonsense somatic *POLI* gene mutations have also been described from various human cancer tissues such as endometrium, large intestine, and lung in the COSMIC database (www.sanger.ac.uk/genetics/CGP/cosmic/), but their functional effects have not been revealed yet. Although we focused on only six selected "putatively functional" coding variants, our biochemical investigation can be a useful initial step to find pol ι variations that have functional impacts and understanding their mechanistic implications. Eleven additional nonsynonymous coding *POLI* variations, located in polymerase core domains and also putatively deleterious, have been added in dbSNP since our study began, and those functional candidates are also under our investigation.

The six germline pol ι variants characterized in this study can be classified into three types according to the changes of relative polymerase efficiencies opposite G and the lesions in the presence of the added metal (Mg^{2+} or Mn^{2+}) compared to wild-type (Tables 2−7). The first type is the defective variant (R96G), which is severely impaired in both Mg^{2+}- and Mn^{2+}-dependent polymerase efficiencies for both normal synthesis and lesion bypass. Surprisingly, this particular variant exhibited a substantial improvement in the Mn^{2+}-dependent N^2-EtG bypass, i.e., large increases (9-fold and 24-fold, respectively) in both efficiency and fidelity for Mn^{2+}-dependent dCTP insertion opposite N^2-EtG compared to wild-type enzyme (Table 5), from which we may speculate the likelihood of a beneficial effect of this variation to efficiently and faithfully bypass such a lesion at the expense of general diminution in polymerase function. The second type is the hyperactive variant (Δ1−25). This N-terminal truncation variant displayed considerable enhancement only in Mg^{2+}-dependent polymerase efficiency but without any alteration in Mn^{2+}-dependent efficiency. The last type is the "wild-type-like" variants (Δ17, I261M, E276K, and Y374N), which retain both normal and TLS polymerase efficiencies similar to those of wild-type in the presence of either Mg^{2+} or Mn^{2+}. The fidelity of nucleotide insertion opposite G and the lesions does not appear to be altered in

most variants except for the R96G variant when compared to wild-type (Tables 2−7). The R96G variant had a reduced fidelity in Mg^{2+}-dependent 8-oxoG bypass due to a greater reduction of insertion efficiency for correct dCTP than for the other nucleotides, as well as an improved fidelity in Mn^{2+}-dependent N^2-EtG bypass (*vide supra*). Although all four studied missense variations (R96G, I261M, E276K, and Y374N) were predicted to be damaging by SIFT and/or PolyPhen, only the former variant was found to be deleterious, but the latter three variants were found to have nearly neutral effects on pol ι function in our study, indicating the substantial false-positive nature of *in silico* prediction. False-positive errors of 20 and 9% have been reported with SIFT and Polyphen, respectively.[42] Taken together, our results suggest the necessity and importance of biochemical approaches to verify the functional alterations in genetic variants, although *in silico* predictions may still be useful for screening putatively damaging genetic variations for functional studies.

Three-dimensional structures of the catalytic core of pol ι have been determined in complex with various DNA substrates with/without incoming nucleotides, which would be useful for the mechanistic understanding of genetic variants (Figure 1).[14,37,38,43−45] The catalytic core of pol ι contains the palm, fingers, thumb, and polymerase-associated domain (PAD) domains, forming the unique narrow active site that is not conducive to Watson−Crick base pairing.[14,44] The mechanistic basis for our finding that the R96G variation caused a severe reduction in pol ι catalytic activity can be explained by a structural role of Arg96 in the active site as previously revealed.[14,44] Thr90, Tyr93, and Arg96 from the fingers domain and Lys239 from the palm domain (the latter three of which are conserved in all Y-family DNA polymerases) function to stabilize the incoming nucleotide by making hydrogen bonds with the triphosphate moiety in the pol ι-DNA-dNTP ternary complex. In particular, Arg96 of pol ι undergoes a substantial conformational change (facing inward) upon nucleotide binding to form hydrogen bonds with the β- and γ-phosphates of the incoming nucleoside triphosphate. Our finding of defective function in the R96G variant is in good agreement with the previous report that Ala substitution of the homologous Arg67 residue in yeast pol η also considerably diminishes its polymerase activity, suggesting that this conserved Arg residue is commonly crucial for catalytic function in Y-family polymerases.[46] However, it is not clear how the R96G variant unexpectedly displays an increased competence in an error-free Mn^{2+}-dependent N^2-EtG bypass. Pol ι normally accommodates the N^2-EtG in the syn conformation paired with incoming dCTP in the active site.[43] The R96G variation abolishes the long and positively charged side chain on Arg96 and thus might lead to an altered conformation that hinders nucleoside triphosphate binding and catalysis for most of the templates but is perhaps well suited only for Mn^{2+}-assisted pairing between a template N^2-EtG (syn) and an incoming dCTP (anti) in the active site pocket.

We established, for the first time, that the Δ1−25 variant (i.e., the former wild-type protein) has a considerably higher Mg^{2+}-dependent polymerase activity (but with no alteration in Mn^{2+}-dependent polymerase activity) and a much higher DNA binding affinity than wild-type pol ι. This unexpected biochemical trait is certainly due to the absence of the N-terminal extension of 25 amino acids (containing 12 acidic residues). As far as we know, all reported pol ι structures have been resolved only from the catalytic core fragment (amino acids 26−445) lacking the N-terminal 25 amino acids, and thus, the structural role of the N-terminal extension is not known yet. However, it is evident from our observations that this negatively charged N-terminal extension can interfere with both DNA substrate binding and Mg^{2+}-dependent polymerase activity of pol ι, but these hindrances can be largely weakened by a low level of Mn^{2+}. Only Mn^{2+} (at low concentration, 150 μM) but not Mg^{2+} seems to considerably overcome the inherently poor DNA binding trait of the wild-type pol ι, possibly by masking or neutralizing the negative charged N-terminal region of this enzyme and thus reducing the potential electrostatic repulsion from the negatively charged phosphosugar backbone of DNA substrates. Pol ι is also known to have a greater preference for Mn^{2+} over Mg^{2+} as a divalent metal for polymerase catalysis and shows maximal polymerase activity at a low concentration of Mn^{2+} (with the optimum around 50−250 μM).[20] Taken together, we can postulate that the wild-type pol ι may require a low level of Mn^{2+} rather than Mg^{2+} as a metal for performing proper polymerase function for two reasons: (i) mediating efficient catalysis and (ii) facilitating tight DNA substrate binding, although the structural basis for such a scenario has not been revealed yet. These biochemical traits of wild-type pol ι are likely to be advantageous in that cells might be able to control the error-prone polymerase function of pol ι by varying the local concentration of metal near DNA damage sites in cell nucleus, which might permit the proficient TLS events by pol ι only in the presence of a low level of Mn^{2+}. Although the intracellular level of Mn^{2+} is physiologically very low (0.1 to 40 μM),[47−49] that of Mn^{2+} could be increased in some pathological cell conditions (e.g., Mn^{2+} overexposure or misregulated Mn^{2+} homeostasis),[50,51] which might stimulate the activity of error-prone pol ι, as well as other Mn^{2+}-dependent DNA-processing enzymes in the nucleus, and thus induce genomic instability. Mn^{2+} has also been known to alter both catalytic efficiency and fidelity of other DNA polymerases including pol β, pol λ, and pol μ, albeit at high concentrations.[52−54] The effects might be related to their active site features with regard to the cofactor Mn^{2+}, which has a slightly smaller ionic radius and a more relaxed coordination than Mg^{2+}, and might allow different interactions with nucleoside triphosphate, DNA, and catalytic residues in the polymerase active site, which could alter polymerase function.[55,56]

It is very conceivable that the cellular pol ι-mediated TLS capacity could be substantially diminished or enhanced in individuals having these two identified dysfunctional *POLI* gene variations. If a cell possessed only the R96G pol ι variant (i.e., homozygote), then most of pol ι-mediated TLS events (except for the increased events of accurate N^2-EtG bypass) would decrease in cells. Conversely, if the cell had only the Δ1−25 pol ι variant, then pol ι-mediated Mg^{2+}-dependent TLS events would increase in cells. We might expect that high replication errors occur with hyperactive pol ι in normal DNA replication because pol ι is inherently error-prone in its general nature. However, predicting how these two *POLI* gene variations would lead to overall TLS-associated mutation outcomes in cells is not straightforward due to the complex TLS properties of pol ι and the cellular existence of other competitive TLS polymerases. Eukaryotic TLS process is carried out not by a single TLS polymerase but by a set of specialized TLS polymerases recruited at a site of DNA damage, although the extent of their individual participation varies depending on the lesion type. The mutation consequence from a particular DNA

lesion in cells can be governed by the total set of enzymatic behavior of multiple TLS polymerases, mainly Y-family polymerases, utilized for the lesion substrate. Unlike Y-family pols η and κ, which are generally considered to be specialized for efficient and error-free bypasses at their cognate lesions, UV-induced pyrimidine dimers and bulky N^2-G adducts, respectively, it is not clear what kind of DNA lesions could be the cognate substrate lesions for pol ι. There is much kinetic and structural evidence suggesting that some DNA lesions such as N^2-EtG, O^6-MeG, 8-oxoG, and abasic sites might be among the favored substrate lesions for pol ι, in that this enzyme can incorporate nucleotides opposite those lesions as efficiently as (or slightly less efficiently than) opposite an unmodified G by utilizing its unique active site and/or Hoogsteen base pairing but with different nucleotide selectivities.[12,17,19,37,38,43,45] Pol ι seems to mediate relatively error-free bypass with some minor-groove N^2-G lesions such as N^2-EtG, while performing a relatively error-prone bypass opposite major-groove O^6-alkylG adducts such as O^6-MeG.[12,17,37,43] In a support of this view, pol ι (as well as pol κ) has been implicated in the error-free bypass of N^2-carboxyMeG and N^2-carboxyEtG lesions in mouse cells.[57] Pol ι has also been implicated to play a protective role from oxidative DNA damage, possibly by mediating both the error-free TLS and the base excision repair of 8-oxoG.[38,58,59] However, the fidelity of 8-oxoG bypass by pol ι seems to be sequence context-dependent because the incorrect dGTP was incorporated more favorably than dCTP opposite template 8-oxoG in our different sequence context as observed here. Experimental evidence support the dual and conflicting "Janus" roles of pol ι in cancers: a protective role of pol ι in mouse lung and skin carcinogenesis[22,23] and a hypermutagenic role of pol ι, upregulated in various human cancer tissues.[24−27] Under these circumstances, it can be hypothesized that individual humans who possess the R96G or the Δ1−25 pol ι variation might have an altered but complex risk for mutation and cancer to various carcinogen exposures, depending on the DNA damage status in their target tissues. In this aspect, it is necessary to perform further studies to verify the *in vivo* impact of those functional pol ι variants in both cellular and organismal contexts. It is also worth examining other nonsynonymous coding variations located in protein interaction domains of pol ι to bind other proteins such as PCNA and ubiquitin, in that they might alter cellular TLS events such as polymerase switching and coordination. It is also plausible that noncoding functional variations in the gene regulatory regions of pol ι might be able to alter pol ι expression levels in cells and thus influence TLS events, although this aspect was out of scope for this study.

In conclusion, our results suggest that two germline genetic variations in human *POLI* gene may either hinder or promote the TLS capability of pol ι with various DNA lesions *in vitro*, possibly leading to different and distinctive mutation phenotypes in genetically affected cells and individuals, i.e., facilitating or protecting against mutagenesis/carcinogenesis after exposure to genotoxic carcinogens. The verification of two dysfunctional genetic variations for human pol ι in this study may provide insight into our understanding of individual differences in cellular TLS capacities to various carcinogen-derived DNA lesions. Such functional genetic alterations in TLS DNA polymerases might be expected to play some part in determining an individual's genomic mutational susceptibility to specific carcinogens and the related cancer risk in human populations, although further *in vivo* or clinical investigations are needed to elucidate these associations.

■ ASSOCIATED CONTENT

Supporting Information

Analysis of human pol ι (1−445) wild-type and variant proteins by SDS-polyacrylamide gel electrophoresis (Figure S1). This material is available free of charge via the Internet at http://pubs.acs.org.

■ AUTHOR INFORMATION

Corresponding Author

*(J.-Y.C.) Tel: +82-31-299-6193. Fax: +82-31-299-6209. E-mail: choijy@skku.edu.

Funding

This work was supported by the Basic Science Research Program through the National Research Foundation of Korea (NRF) funded by the Ministry of Education, Science and Technology (Grant 2012R1A1A2042391) (to J.-Y.C.), Samsung Biomedical Research Institute grant, #SBRI SMX1132091 (to J.-Y.C.), and the National Institutes of Health Grants R01 CA183895 (to R.L.E.) and R01 ES010375 (to F.P.G.).

Notes

The authors declare no competing financial interest.

■ ABBREVIATIONS

A, adenine; BSA, bovine serum albumin; C, cytosine; Et, ethyl; FAM, 6-carboxyfluorescein; G, guanine; Me, methyl; 8-oxoG, 8-oxo-7,8-dihydroG; PCR, polymerase chain reaction; pol, DNA polymerase; SDS, sodium dodecyl sulfate; T, thymine; TLS, translesion synthesis

■ REFERENCES

(1) Friedberg, E. C., Walker, G. C., Siede, W., Wood, R. D., Schultz, R. A., and Ellenberger, T. (2006) *DNA Repair And Mutagenesis*, 2nd ed., American Society for Microbiology Press, Washington, D.C.

(2) Giglia-Mari, G., Zotter, A., and Vermeulen, W. (2011) DNA damage response. *Cold Spring Harb. Perspect. Biol. 3*, a000745.

(3) Hoeijmakers, J. H. (2009) DNA damage, aging, and cancer. *N. Engl. J. Med. 361*, 1475−1485.

(4) Jackson, S. P., and Bartek, J. (2009) The DNA-damage response in human biology and disease. *Nature 461*, 1071−1078.

(5) Kennedy, D. O., Agrawal, M., Shen, J., Terry, M. B., Zhang, F. F., Senie, R. T., Motykiewicz, G., and Santella, R. M. (2005) DNA repair capacity of lymphoblastoid cell lines from sisters discordant for breast cancer. *J. Natl. Cancer Inst. 97*, 127−132.

(6) Gorlova, O. Y., Weng, S. F., Zhang, Y., Amos, C. I., Spitz, M. R., and Wei, Q. (2008) DNA repair capacity and lung cancer risk in never smokers. *Cancer Epidemiol. Biomarkers Prev. 17*, 1322−1328.

(7) Wang, L. E., Gorlova, O. Y., Ying, J., Qiao, Y., Weng, S. F., Lee, A. T., Gregersen, P. K., Spitz, M. R., Amos, C. I., and Wei, Q. (2013) Genome-wide association study reveals novel genetic determinants of DNA repair capacity in lung cancer. *Cancer Res. 73*, 256−264.

(8) Alberg, A. J., Jorgensen, T. J., Ruczinski, I., Wheless, L., Shugart, Y. Y., Berthier-Schaad, Y., Kessing, B., Hoffman-Bolton, J., Helzlsouer, K. J., Kao, W. H., Francis, L., Alani, R. M., Smith, M. W., and Strickland, P. T. (2013) DNA repair gene variants in relation to overall cancer risk: a population-based study. *Carcinogenesis 34*, 86−92.

(9) Choi, J.-Y., Eoff, R. E., and Guengerich, F. P. (2011) Bypass DNA polymerases, In *Chemical Carcinogenesis* (Penning, T. M., Ed.) pp 345−373, Humana Press, New York.

(10) Choi, J.-Y., Angel, K. C., and Guengerich, F. P. (2006) Translesion synthesis across bulky N^2-alkyl guanine DNA adducts by human DNA polymerase κ. *J. Biol. Chem. 281*, 21062−21072.

(11) Choi, J.-Y., and Guengerich, F. P. (2005) Adduct size limits efficient and error-free bypass across bulky N^2-guanine DNA lesions by human DNA polymerase η. *J. Mol. Biol. 352*, 72−90.

(12) Choi, J.-Y., and Guengerich, F. P. (2006) Kinetic evidence for inefficient and error-prone bypass across bulky N^2-guanine DNA adducts by human DNA polymerase ι. *J. Biol. Chem. 281*, 12315−12324.
(13) Choi, J.-Y., and Guengerich, F. P. (2008) Kinetic analysis of translesion synthesis opposite bulky N^2- and O^6-alkylguanine DNA adducts by human DNA polymerase REV1. *J. Biol. Chem. 283*, 23645−23655.
(14) Nair, D. T., Johnson, R. E., Prakash, S., Prakash, L., and Aggarwal, A. K. (2004) Replication by human DNA polymerase-iota occurs by Hoogsteen base-pairing. *Nature 430*, 377−380.
(15) Choi, J.-Y., Lim, S., Eoff, R. L., and Guengerich, F. P. (2009) Kinetic analysis of base-pairing preference for nucleotide incorporation opposite template pyrimidines by human DNA polymerase ι. *J. Mol. Biol. 389*, 264−274.
(16) Kirouac, K. N., and Ling, H. (2009) Structural basis of error-prone replication and stalling at a thymine base by human DNA polymerase iota. *EMBO J. 28*, 1644−1654.
(17) Choi, J.-Y., Chowdhury, G., Zang, H., Angel, K. C., Vu, C. C., Peterson, L. A., and Guengerich, F. P. (2006) Translesion synthesis across O^6-alkylguanine DNA adducts by recombinant human DNA polymerases. *J. Biol. Chem. 281*, 38244−38256.
(18) Vaisman, A., Frank, E. G., Iwai, S., Ohashi, E., Ohmori, H., Hanaoka, F., and Woodgate, R. (2003) Sequence context-dependent replication of DNA templates containing UV-induced lesions by human DNA polymerase iota. *DNA Repair 2*, 991−1006.
(19) Choi, J.-Y., Lim, S., Kim, E. J., Jo, A., and Guengerich, F. P. (2010) Translesion synthesis across abasic lesions by human B-family and Y-family DNA polymerases alpha, delta, eta, iota, kappa, and REV1. *J. Mol. Biol. 404*, 34−44.
(20) Frank, E. G., and Woodgate, R. (2007) Increased catalytic activity and altered fidelity of human DNA polymerase ι in the presence of manganese. *J. Biol. Chem. 282*, 24689−24696.
(21) Dumstorf, C. A., Clark, A. B., Lin, Q., Kissling, G. E., Yuan, T., Kucherlapati, R., McGregor, W. G., and Kunkel, T. A. (2006) Participation of mouse DNA polymerase iota in strand-biased mutagenic bypass of UV photoproducts and suppression of skin cancer. *Proc. Natl. Acad. Sci. U.S.A. 103*, 18083−18088.
(22) Ohkumo, T., Kondo, Y., Yokoi, M., Tsukamoto, T., Yamada, A., Sugimoto, T., Kanao, R., Higashi, Y., Kondoh, H., Tatematsu, M., Masutani, C., and Hanaoka, F. (2006) UV-B radiation induces epithelial tumors in mice lacking DNA polymerase eta and mesenchymal tumors in mice deficient for DNA polymerase iota. *Mol. Cell. Biol. 26*, 7696−7706.
(23) Iguchi, M., Osanai, M., Hayashi, Y., Koentgen, F., and Lee, G. H. (2014) The error-prone DNA polymerase iota provides quantitative resistance to lung tumorigenesis and mutagenesis in mice. *Oncogene 33*, 3612−3617.
(24) Yang, J., Chen, Z., Liu, Y., Hickey, R. J., and Malkas, L. H. (2004) Altered DNA polymerase iota expression in breast cancer cells leads to a reduction in DNA replication fidelity and a higher rate of mutagenesis. *Cancer Res. 64*, 5597−5607.
(25) Zhou, J., Zhang, S., Xie, L., Liu, P., Xie, F., Wu, J., Cao, J., and Ding, W. Q. (2012) Overexpression of DNA polymerase iota (Poliota) in esophageal squamous cell carcinoma. *Cancer Sci. 103*, 1574−1579.
(26) Albertella, M. R., Lau, A., and O'Connor, M. J. (2005) The overexpression of specialized DNA polymerases in cancer. *DNA Repair 4*, 583−593.
(27) Yuan, F., Xu, Z., Yang, M., Wei, Q., Zhang, Y., Yu, J., Zhi, Y., Liu, Y., Chen, Z., and Yang, J. (2013) Overexpressed DNA polymerase iota regulated by JNK/c-Jun contributes to hypermutagenesis in bladder cancer. *PLoS One 8*, e69317.
(28) Luedeke, M., Linnert, C. M., Hofer, M. D., Surowy, H. M., Rinckleb, A. E., Hoegel, J., Kuefer, R., Rubin, M. A., Vogel, W., and Maier, C. (2009) Predisposition for TMPRSS2-ERG fusion in prostate cancer by variants in DNA repair genes. *Cancer Epidemiol. Biomarkers Prev. 18*, 3030−3035.
(29) Sakiyama, T., Kohno, T., Mimaki, S., Ohta, T., Yanagitani, N., Sobue, T., Kunitoh, H., Saito, R., Shimizu, K., Hirama, C., Kimura, J., Maeno, G., Hirose, H., Eguchi, T., Saito, D., Ohki, M., and Yokota, J. (2005) Association of amino acid substitution polymorphisms in DNA repair genes TP53, POLI, REV1 and LIG4 with lung cancer risk. *Int. J. Cancer 114*, 730−737.
(30) Ng, P. C., and Henikoff, S. (2001) Predicting deleterious amino acid substitutions. *Genome Res. 11*, 863−874.
(31) Ramensky, V., Bork, P., and Sunyaev, S. (2002) Human non-synonymous SNPs: server and survey. *Nucleic Acids Res. 30*, 3894−3900.
(32) Adzhubei, I. A., Schmidt, S., Peshkin, L., Ramensky, V. E., Gerasimova, A., Bork, P., Kondrashov, A. S., and Sunyaev, S. R. (2010) A method and server for predicting damaging missense mutations. *Nat. Methods 7*, 248−249.
(33) Choi, J.-Y., and Guengerich, F. P. (2004) Analysis of the effect of bulk at N^2-alkylguanine DNA adducts on catalytic efficiency and fidelity of the processive DNA polymerases bacteriophage T7 exonuclease- and HIV-1 reverse transcriptase. *J. Biol. Chem. 279*, 19217−19229.
(34) Boosalis, M. S., Petruska, J., and Goodman, M. F. (1987) DNA polymerase insertion fidelity: gel assay for site-specific kinetics. *J. Biol. Chem. 262*, 14689−14696.
(35) Song, I., Kim, E. J., Kim, I. H., Park, E. M., Lee, K. E., Shin, J. H., Guengerich, F. P., and Choi, J.-Y. (2014) Biochemical characterization of eight genetic variants of human DNA polymerase κ involved in error-free bypass across bulky N^2-guanyl DNA adducts. *Chem. Res. Toxicol. 27*, 919−930.
(36) Ketkar, A., Zafar, M. K., Maddukuri, L., Yamanaka, K., Banerjee, S., Egli, M., Choi, J.-Y., Lloyd, R. S., and Eoff, R. L. (2013) Leukotriene biosynthesis inhibitor MK886 impedes DNA polymerase activity. *Chem. Res. Toxicol. 26*, 221−232.
(37) Pence, M. G., Choi, J.-Y., Egli, M., and Guengerich, F. P. (2010) Structural basis for proficient incorporation of dTTP opposite O^6-methylguanine by human DNA polymerase ι. *J. Biol. Chem. 285*, 40666−40672.
(38) Kirouac, K. N., and Ling, H. (2011) Unique active site promotes error-free replication opposite an 8-oxo-guanine lesion by human DNA polymerase iota. *Proc. Natl. Acad. Sci. U.S.A. 108*, 3210−3215.
(39) Manolio, T. A., Collins, F. S., Cox, N. J., Goldstein, D. B., Hindorff, L. A., Hunter, D. J., McCarthy, M. I., Ramos, E. M., Cardon, L. R., Chakravarti, A., Cho, J. H., Guttmacher, A. E., Kong, A., Kruglyak, L., Mardis, E., Rotimi, C. N., Slatkin, M., Valle, D., Whittemore, A. S., Boehnke, M., Clark, A. G., Eichler, E. E., Gibson, G., Haines, J. L., Mackay, T. F., McCarroll, S. A., and Visscher, P. M. (2009) Finding the missing heritability of complex diseases. *Nature 461*, 747−753.
(40) Nelson, M. R., Wegmann, D., Ehm, M. G., Kessner, D., St. Jean, P., Verzilli, C., Shen, J., Tang, Z., Bacanu, S. A., Fraser, D., Warren, L., Aponte, J., Zawistowski, M., Liu, X., Zhang, H., Zhang, Y., Li, J., Li, Y., Li, L., Woollard, P., Topp, S., Hall, M. D., Nangle, K., Wang, J., Abecasis, G., Cardon, L. R., Zollner, S., Whittaker, J. C., Chissoe, S. L., Novembre, J., and Mooser, V. (2012) An abundance of rare functional variants in 202 drug target genes sequenced in 14,002 people. *Science 337*, 100−104.
(41) Zhu, Q., Ge, D., Maia, J. M., Zhu, M., Petrovski, S., Dickson, S. P., Heinzen, E. L., Shianna, K. V., and Goldstein, D. B. (2011) A genome-wide comparison of the functional properties of rare and common genetic variants in humans. *Am. J. Hum. Genet. 88*, 458−468.
(42) Ng, P. C., and Henikoff, S. (2006) Predicting the effects of amino acid substitutions on protein function. *Annu. Rev. Genomics Hum. Genet. 7*, 61−80.
(43) Pence, M. G., Blans, P., Zink, C. N., Hollis, T., Fishbein, J. C., and Perrino, F. W. (2009) Lesion bypass of N^2-ethylguanine by human DNA polymerase ι. *J. Biol. Chem. 284*, 1732−1740.
(44) Nair, D. T., Johnson, R. E., Prakash, L., Prakash, S., and Aggarwal, A. K. (2006) An incoming nucleotide imposes an anti to syn conformational change on the templating purine in the human DNA polymerase-iota active site. *Structure 14*, 749−755.

(45) Nair, D. T., Johnson, R. E., Prakash, L., Prakash, S., and Aggarwal, A. K. (2009) DNA synthesis across an abasic lesion by human DNA polymerase iota. *Structure 17*, 530−537.
(46) Johnson, R. E., Trincao, J., Aggarwal, A. K., Prakash, S., and Prakash, L. (2003) Deoxynucleotide triphosphate binding mode conserved in Y family DNA polymerases. *Mol. Cell. Biol. 23*, 3008−3012.
(47) Ash, D. E., and Schramm, V. L. (1982) Determination of free and bound manganese(II) in hepatocytes from fed and fasted rats. *J. Biol. Chem. 257*, 9261−9264.
(48) Markesbery, W. R., Ehmann, W. D., Alauddin, M., and Hossain, T. I. (1984) Brain trace element concentrations in aging. *Neurobiol. Aging 5*, 19−28.
(49) Versieck, J. (1985) Trace elements in human body fluids and tissues. *Crit. Rev. Clin. Lab. Sci. 22*, 97−184.
(50) Crossgrove, J., and Zheng, W. (2004) Manganese toxicity upon overexposure. *NMR Biomed. 17*, 544−553.
(51) Garcia-Rodriguez, N., Diaz de la Loza Mdel, C., Andreson, B., Monje-Casas, F., Rothstein, R., and Wellinger, R. E. (2012) Impaired manganese metabolism causes mitotic misregulation. *J. Biol. Chem. 287*, 18717−18729.
(52) Wang, T. S., Eichler, D. C., and Korn, D. (1977) Effect of Mn^{2+} on the in vitro activity of human deoxyribonucleic acid polymerase beta. *Biochemistry 16*, 4927−4934.
(53) Blanca, G., Shevelev, I., Ramadan, K., Villani, G., Spadari, S., Hübscher, U., and Maga, G. (2003) Human DNA polymerase lambda diverged in evolution from DNA polymerase beta toward specific Mn(++) dependence: a kinetic and thermodynamic study. *Biochemistry 42*, 7467−7476.
(54) Dominguez, O., Ruiz, J. F., Lain de Lera, T., Garcia-Diaz, M., Gonzalez, M. A., Kirchhoff, T., Martinez, A. C., Bernad, A., and Blanco, L. (2000) DNA polymerase mu (Pol mu), homologous to TdT, could act as a DNA mutator in eukaryotic cells. *EMBO J. 19*, 1731−1742.
(55) Pelletier, H., Sawaya, M. R., Wolfle, W., Wilson, S. H., and Kraut, J. (1996) Crystal structures of human DNA polymerase β complexed with DNA: implications for catalytic mechanism, processivity, and fidelity. *Biochemistry 35*, 12742−12761.
(56) Yang, W., Lee, J. Y., and Nowotny, M. (2006) Making and breaking nucleic acids: two-Mg^{2+}-ion catalysis and substrate specificity. *Mol. Cell 22*, 5−13.
(57) Yuan, B., You, C., Andersen, N., Jiang, Y., Moriya, M., O'Connor, T. R., and Wang, Y. (2011) The roles of DNA polymerases κ and ι in the error-free bypass of N2-carboxyalkyl-2′-deoxyguanosine lesions in mammalian cells. *J. Biol. Chem. 286*, 17503−17511.
(58) Kirouac, K. N., and Ling, H. (2011) Poli: Shining light on repair of oxidative DNA lesions and mutations. *Cell Cycle 10*, 1520−1521.
(59) Petta, T. B., Nakajima, S., Zlatanou, A., Despras, E., Couve-Privat, S., Ishchenko, A., Sarasin, A., Yasui, A., and Kannouche, P. (2008) Human DNA polymerase iota protects cells against oxidative stress. *EMBO J. 27*, 2883−2895.
(60) Ren, J., Wen, L., Gao, X., Jin, C., Xue, Y., and Yao, X. (2009) DOG 1.0: illustrator of protein domain structures. *Cell Res. 19*, 271−273.